REVIEW

Cardiac Alternans: From Bedside to Bench and Back

Zhilin Qu(iD), James N. Weiss(iD)

ABSTRACT: Cardiac alternans arises from dynamical instabilities in the electrical and calcium cycling systems of the heart, and often precedes ventricular arrhythmias and sudden cardiac death. In this review, we integrate clinical observations with theory and experiment to paint a holistic portrait of cardiac alternans: the underlying mechanisms, arrhythmic manifestations and electrocardiographic signatures. We first summarize the cellular and tissue mechanisms of alternans that have been demonstrated both theoretically and experimentally, including 3 voltage-driven and 2 calcium-driven alternans mechanisms. Based on experimental and simulation results, we describe their relevance to mechanisms of arrhythmogenesis under different disease conditions, and their link to electrocardiographic characteristics of alternans observed in patients. Our major conclusion is that alternans is not only a predictor, but also a causal mechanism of potentially lethal ventricular and atrial arrhythmias across the full spectrum of arrhythmia mechanisms that culminate in functional reentry, although less important for anatomic reentry and focal arrhythmias.

Key Words: atrial fibrillation ■ Brugada syndrome ■ cardiovascular diseases ■ long QT syndrome ■ myocardial ischemia ■ torsades de pointes ■ ventricular fibrillation

In 1872, German physician Ludwig Traube published his observations on a patient with alcoholic cardio-myopathy and heart failure whose pulse alternated in intensity from beat to beat (pulsus alternans), presaging his sudden death only 2 months later[1]. After the invention of the electrocardiogram, Herring in 1909 reported alternans of both the QRS complex (QRSA) and T-wave (TWA) in animal experiments,[2] and established a link between electrical and mechanical (pulsus) alternans, confirmed in humans a year later by Lewis.[3] Over the past 150 years, mechanical pulsus alternans and electrical alternans have been observed in many settings in which arrhythmias are common, including heart failure, acute and chronic myocardial ischemia, cardiomyopathy, inherited arrhythmia syndromes, and drug and electrolyte disturbances. Extensive clinical, experimental, and theoretical studies have been carried out to elucidate the mechanisms of alternans and its links to arrhythmias and sudden cardiac death[4–14] (searching PubMed with "alternans, cardiac" returned 2329 articles dating from 1947 to 2022). In the 1990s, human clinical trials conclusively established the link between electrocardiographic TWA and arrhythmia risk.[13,15,16] In long QT syndromes (LQTS), TWA prevalence and arrhythmia risk increase in parallel with the corrected QT intervals (Figure 1A).[17] Moreover, clinical observations suggest that TWA is more than just a predictor of arrhythmia risk, but may also be a causal mechanism. For example, there are many published examples from LQTS patients in which TWA immediately precedes the onset of its signature arrhythmia, Torsade de pointes (Figure 1 B and C).[18–23] On the other hand, many episodes of Torsade de pointes also occur without immediately preceding TWA, often following a short-long-short sequence (Figure 1D).[24–26] Today, macroscopic TWA is used in assessing arrhythmia risk in patients with LQTS,[27] and microvolt TWA test is used for risk stratification for patients with heart failure.[28,29]

Nonstandard Abbreviations and Acronyms

AF	atrial fibrillation
APD	action potential duration
APDR	action potential duration restitution
CaT	calcium transient
CPVT	catecholaminergic polymorphic ventricular tachycardia
CVR	conduction velocity restitution
DAD	delayed afterdepolarization
DI	diastolic interval
EAD	early afterdepolarization
I_{to}	transient outward potassium current
LCC	L-type calcium channel
LQTS	long QT syndrome
PVC	premature ventricular complex
QRSA	QRS alternans
RyR	ryanodine receptor
SERCA	sarco-endoplasmic reticulum calcium ATPase
SDA	spatially discordant alternans
SR	sarcoplasmic reticulum
TQ	time interval between the T-wave and the next Q-wave
TWA	T-wave alternans
VT	ventricular tachycardia

In this review article, our goal is to provide a holistic portrait of cardiac alternans and its relationship to cardiac arrhythmias by linking the relevant clinical observations to experiments and theory, focusing primarily on life-threatening ventricular arrhythmias but also including atrial arrhythmias. We begin by summarizing the cellular and tissue mechanisms of alternans that have been demonstrated theoretically and experimentally, including voltage-driven and calcium (Ca)-driven mechanisms, and their involvement in the dynamics of arrhythmia initiation. We link these mechanisms to the electrocardiogram characteristics of alternans observed in patients under various pathophysiological conditions. Based on experimental and simulation results, we discuss the relevance of alternans to arrhythmogenesis across a spectrum of disease states, distinguishing between alternans as a predictor versus a direct causal factor. We conclude by discussing alternans in risk stratification and as a therapeutic target for preventative therapies.

CELLULAR MECHANISMS OF ALTERNANS

As an excitable medium, the heart is a dynamical system capable of exhibiting a wide range of spontaneously self-organizing behaviors, from pacemaking driving the normal heartbeat to pathophysiological phenomena such as triggered activity and reentry. Alternans falls within this spectrum of behaviors, and can be precipitated by a variety of conditions, including changes in heart rate, genetic or post-translational changes in ionic current conductances or kinetics, altered intracellular Ca loading and sarcoplasmic reticulum (SR) Ca release properties, etc. In this article, we use the term repolarization alternans to refer to both TWA and action potential duration (APD) alternans, since APD is the major determinant of the T-wave and QT interval. Likewise, we use the term mechanical alternans to refer equivalently to pulsus alternans and intracellular Ca transient (CaT) alternans, since the CaT is the major determinant of contractile strength.

From a dynamical systems viewpoint, cardiac arrhythmias can be classified into 3 major categories[30]: Ca cycling disorders (typified by catecholaminergic polymorphic ventricular tachycardia [CPVT]), prolonged repolarization disorders (typified by LQTS), and early repolarization disorders (typified by Brugada and short QT syndromes). As opposed to inherited arrhythmia syndromes, the more common complex diseases associated with lethal ventricular tachycardia (VT) and ventricular fibrillation generally involve more than a single category. For example, chronic heart failure involves both abnormal Ca cycling and prolonged repolarization, and acute ischemia involves both abnormal Ca cycling and early repolarization. Alternans is a feature common to all 3 arrhythmia categories.

The first rigorous theory of repolarization alternans was developed in 1968 by Nolasco and Dahlen[31] who showed that in frog heart, the occurrence of APD alternans is determined by the slope of the APD restitution (APDR) curve. Since then, new theories and mechanisms of alternans have been uncovered through rigorous theoretical analysis confirmed by computer simulations and supported by experimental and clinical observations. Alternans can be generally subdivided into voltage-driven mechanisms and Ca-driven mechanisms, related to the fact that the heart contains 2 excitable subsystems, the voltage subsystem supporting electrical wave propagation through cardiac tissue and the Ca-induced Ca release subsystem supporting Ca wave propagation within cardiac cells. Each subsystem is capable of generating alternans and more complex dynamical phenomena such as spiral/scroll wave reentry on its own. In voltage-driven alternans, APD dynamics drive repolarization alternans with mechanical alternans following passively, reflecting the fact that the APD is an important factor regulating CaT amplitude. In Ca-driven alternans, intracellular Ca dynamics drive mechanical alternans and repolarization alternans follows passively, since the CaT amplitude feeds back to influence APD via its effects on Ca-sensitive ionic conductances such as the L-type Ca
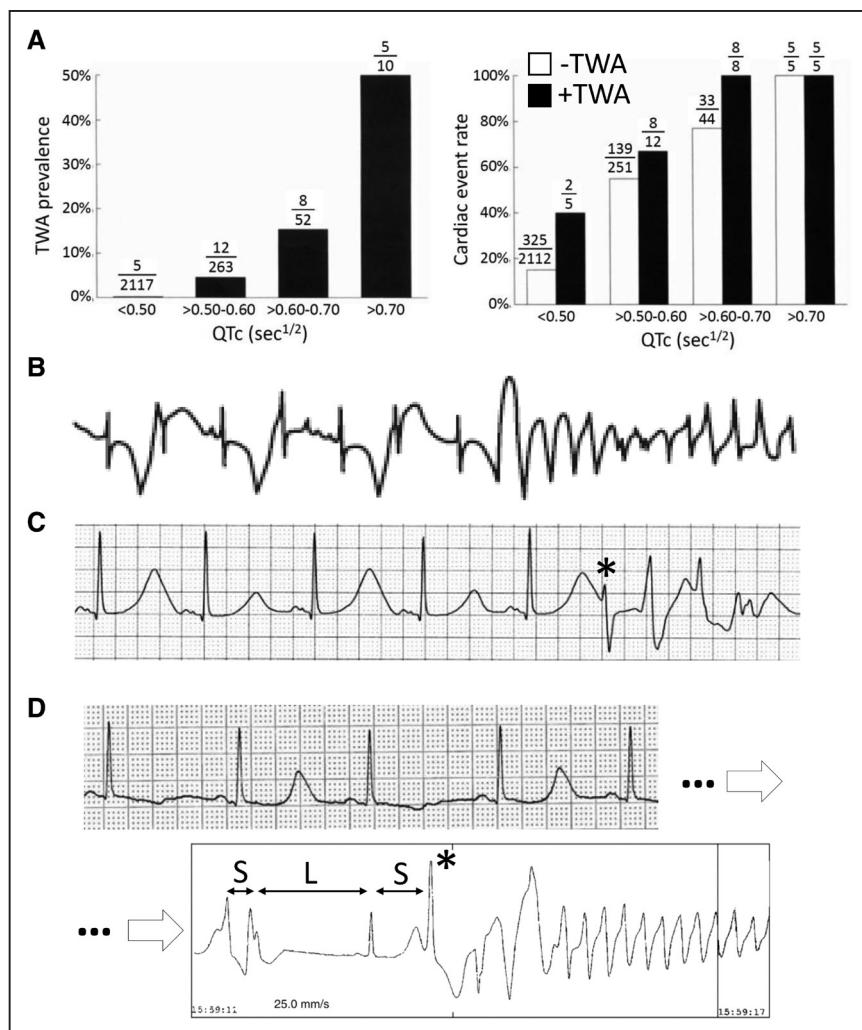
Figure 1. T-wave alternans (TWA) and arrhythmogenesis.
A, TWA prevalence and arrhythmias in long QT syndrome (LQTS) patients.[17] **Left**, TWA prevalence vs corrected QT interval (QTc). **Right**, Cardiac event rate vs QTc with (black) and without (white) TWA. **B**, TWA transitioning directly to Torsade de pointes (TdP) without a clear preceding premature ventricular complex (PVC).[11] **C**, TWA in which TdP is initiated by a PVC falling on the large T-wave of the alternating beats.[23] **D**, TWA, followed sometime later by TdP initiated by a short-long-short sequence.[24]

current, electrogenic Na-Ca exchanger, and Ca-activated currents. However, since the voltage and Ca subsystems are inherently bidirectionally coupled via the effects of intracellular Ca on ionic conductances controlling membrane voltage and vice versa, the 2 subsystems always exert joint influences on each other, which can be synergistic or antagonistic depending on underlying conditions. From a practical standpoint, this means that when both voltage and Ca subsystems are free-running, alternans is never purely voltage-driven or purely Ca-driven; only their relative predominance varies.

Voltage-Driven Alternans

Voltage-driven alternans can be classified into 3 submechanisms[12,32]: (1) alternans driven by a steep APDR slope at fast heart rates or short diastolic intervals (DI), as originally described by Nolasco and Dahlen[31]; (2) alternans driven by factors prolonging repolarization such as early afterdepolarizations (EAD) in LQTS; and (3) alternans driven by all-or-none early repolarization as in Brugada and short QT syndromes. In all 3 cases, the features of the APDR curve play a critical role (Figure 2).

Steep APDR slope-induced APD alternans
The APDR curve can be measured experimentally by the extrastimulus method (ie, pacing heart tissue at a fixed pacing interval [S1S1] and introducing timed extrastimuli [S1S2] at different DIs), or by the rapid pacing method (ie, pacing the heart tissue at incrementally faster rates to shorten the DI until 1:1 capture is lost). In both cases, the APDR curve is then obtained by plotting APD as a function of the preceding DI. The resulting APDR curve represents the collective behavior of the recovery kinetics of the ionic currents that are active during the action potential. Depending on its recovery time constants, each ionic current contributes to a different DI range.[33] Na channels recover quickly and thus affect APDR at short DIs (although their recovery kinetics are slowed by acute ischemia due to the depolarized resting potential, Na channel remodeling or drugs). L-type Ca channels (LCCs) recover more slowly than Na channels, affecting APDR at short to intermediate DIs, and time-dependent K channels recover even more slowly, affecting ADPR over intermediate to long DIs. In general, APD prolongs monotonically as DI increases

(Figure 2A, middle), but non-monotonic responses can also occur.[34]

The ADPR curve can be represented mathematically by the equation

$$APD_{n+1} = f(DI_n) \qquad (1)$$

such that once the function $f(DI)$ is obtained from the experimental data, one can predict APD_{n+1} for any DI_n. In 1968, Nolasco and Dahlen[31] used a graphic representation of this iterative process to show that persistent APD alternans developed in frog hearts when the slope of the APDR curve exceeded 1 at the point of its intersection with the pacing cycle length line (Figure 2A, middle).[12] Since the APDR slope generally becomes steeper as heart rate increases, this mechanism of alternans is generally promoted by fast heart rates (but can occur at normal or slow heart rates when APD is long enough so that the DI is short, as illustrated by the example in the left of Figure 2A). This elegant analysis in the frog heart, however, has only partial relevance to the mammalian heart, for 2 reasons. First, the frog heart has a very limited intracellular Ca cycling system due to its rudimentary SR compared with mammalian hearts.[35] In normal mammalian heart, however, Ca-driven alternans plays a much greater role in initiating APD alternans as heart rate increases, which typically occurs well before the APDR slope exceeds one in experiments.[36–39] Second, the APDR slope >1 criterion is strictly valid only if APD is solely a function of the previous DI, as indicated by Equation 1. If short-term memory is present (due to ionic currents with very slow kinetic components or slow heart rate-dependent intracellular ion accumulation/depletion kinetics) such that the APD is also influenced by the pacing history prior to the last DI, then the APDR slope >1 criterion for instability no longer holds. This is the case in mammalian hearts, since the APDR curve obtained by the extrastimulus method differs when the baseline pacing rate is changed, and also differs from that obtained by the rapid pacing method.[34,37,40] Thus, in the presence of short-term memory, the APDR curve is not unique, and depends on the pacing protocol and history.[34,37,40] Theoretically, it is possible to include the short-term memory effects to assess more precisely the role of the APDR on the genesis of APD alternans, and when done,[41] an even steeper APDR slope is generally required for alternans to occur.

EAD-induced alternans

EADs are an all-or-none phenomenon associated with APD prolongation due to reduced repolarization reserve,[42,43] and at some heart rates exhibit an alternating pattern in which an EAD prolongs the APD of every other beat (Figure 2B, left).[20,44,45] The transition to alternans is related to the sudden sharp jump in the APDR curve typically occurring at long DIs due to the all-or-none occurrence of EADs (Figure 2B, middle).

The dynamical mechanism of alternans can still be illustrated by the same graphical method. However, the APDR slope >1 criterion for the onset of alternans is not strictly valid because short-term memory effects also play a key role, which can be mathematically solved using iterative maps.[12,46] Differing from steep APDR slope-induced alternans, EAD-induced alternans is generally promoted by normal or slow heart rates and suppressed by fast heart rates (Figure 2B, right).[32,47] Theoretically, APD alternans can also occur when APD is very long without the presence of EADs, induced by steep APDR at normal or slow heart rates with either very short DIs as in Figure 2A or long DIs.[48]

Early repolarization-induced alternans

In regions of the heart with a high density of transient outward K current (I_{to}) or other I_{to}-like currents, the action potential often takes on a spike-and-dome appearance that is sensitive to all-or-none repolarization in which the action potential dome suddenly disappears, leaving only the initial spike with a very short APD (Figure 2C, left). Similar to the EAD case, APD alternans can be illustrated graphically as arising from the steep APDR slope reflecting the interaction between I_{to}-induced early repolarization and the slow recovery kinetics of the slow delayed rectifier K current[46] (Figure 2C, middle). As with EAD-induced alternans, however, rigorous analysis of the onset of alternans requires iterative map approaches integrating the short-term memory effects.[46] Early repolarization-induced alternans has been demonstrated experimentally in mammalian ventricular tissue[49–51] as well as computer simulations,[12,52,53] and typically occurs at normal to elevated heart rates (Figure 2C, right).

Complex behaviors and chaos

In all 3 voltage-driven alternans mechanisms described above, it is the steep regions of the APDR curve that play the key causal roles in generating APD alternans. Moreover, in all 3 cases, alternans is a precursor to more complex behaviors, such as higher order periodicity and chaos. In the steep APDR slope case, fast heart rates leading to loss of 1:1 capture can lead to n:m capture (ie, Wenckebach phenomenon) manifested in higher order periodicity and chaos.[12,54–56] In this case, complex APD behaviors only occur after 1:1 capture is lost (Figure 2A, right). In contrast, for both the EAD and early repolarization cases, higher order periodicity and chaos can occur without loss of 1:1 capture, as indicated by the regions with multiple APD values at the same pacing cycle length in the right of Figure 2B and 2C.[32,44–47,49] The dynamical mechanisms of these complex behaviors have also been rigorously analyzed using iterative map approaches,[44,46] which show that short-term memory plays a key role. Thus, both alternans and more complex behaviors originate from the same APDR-induced instabilities, with the alternans being an early prognosticator of more complex instabilities to come.[57]
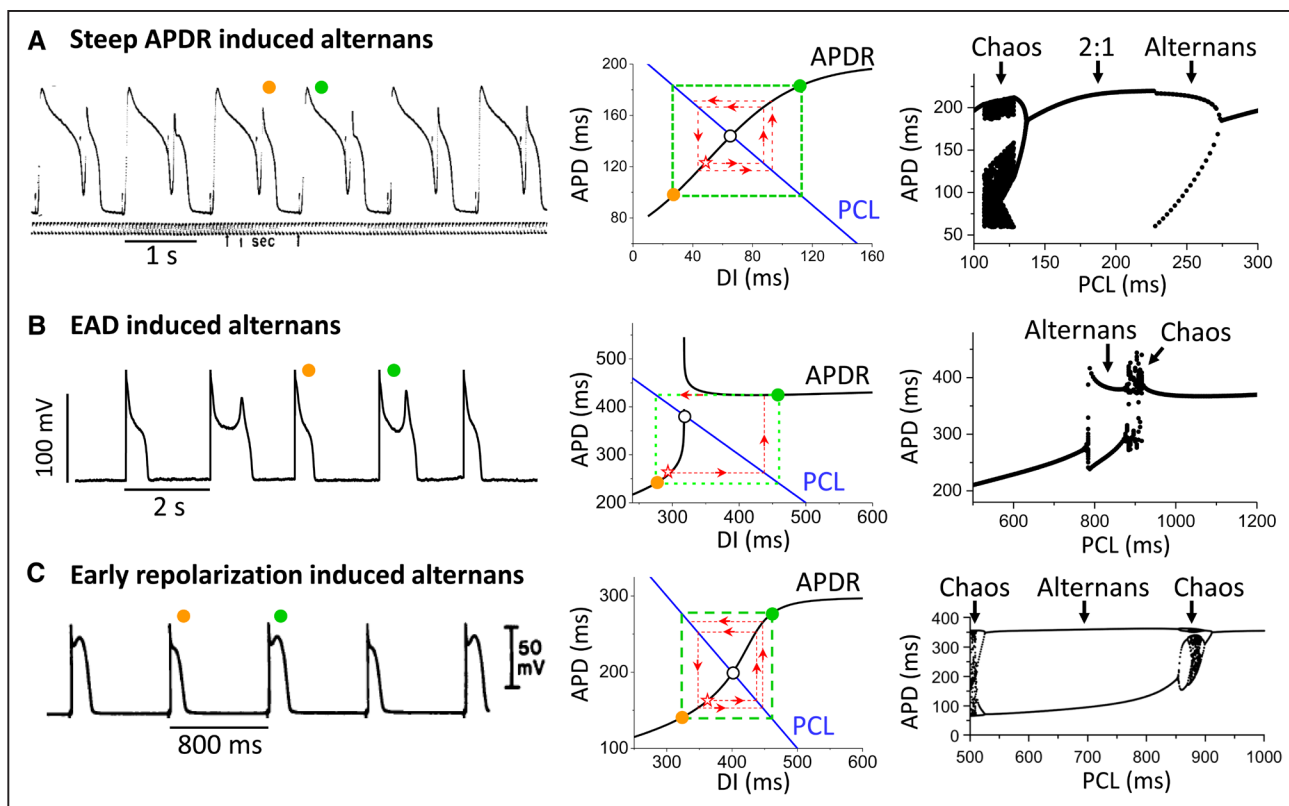
Figure 2. Voltage-driven alternans.
A, Steep action potential duration restitution (APDR)-slope–induced action potential duration (APD) alternans. **B**, Early afterdepolarization (EAD)-induced APD alternans. **C**, Early repolarization-induced APD alternans. **Left**, Experimental action potential (AP) recordings for the 3 cases, obtained from frog ventricle by Nolasco and Dhalen (**A**),[31] a rabbit ventricular myocyte with hypokalemia-induced EADs (**B**),[45] and canine epicardial ventricular muscle during simulated ischemia-induced early repolarization (**C**).[49] **Middle**, APDR curves for the 3 cases obtained from corresponding computer simulations.[12,32,47] The intersection of the APDR curve (black) and pacing cycle length (PCL) line (blue) is the equilibrium point (open circle). If the slope of the APDR curve at this point is >1, the equilibrium point is unstable. Using the graphical cobweb approach pioneered by Nolasco and Dhalen,[31] starting from an initial APD and diastolic interval (DI; star symbol), the subsequent APD and DI values alternate in a growing pattern (red dashed lines and arrows), eventually reaching steady-state APD alternans (green dashed box and colored circles). **Right**, Corresponding plots of APD versus PCL for the 3 cases.[12,32,47] For each PCL, more than 20 consecutive APDs are superimposed. Two APD values at the same PCL indicate alternans, and many APD values indicate high periodicity or chaos.

Ca-Driven Alternans

Just as the heart is an excitable system designed to initiate a coordinated contraction/relaxation cycle by propagating the action potential from myocyte to myocyte, each myocyte's internal Ca cycling system is an excitable subsystem in its own right, in which the Ca flowing through LCCs during the action potential activates the release of a large amount of intracellular Ca stored in the SR via Ca-induced Ca release (Figure 3A through 3C). Under the appropriate conditions, the CaT can exhibit spontaneous alternans on its own, even when the action potential waveform is voltage-clamped to prevent voltage-driven APD alternans from interfering (Figure 3D).[58–61]

The mechanism of Ca-driven alternans is more complex than voltage-driven alternans, due to the complex spatial arrangement of the network of intracellular Ca release units (CRUs) within each myocyte's cytoplasm (Figure 3B).[62] Within the CRU network, each CRU consists of a cluster of Ca release channels called ryanodine receptors (RyRs) residing in the SR membrane that are closely apposed to a cluster of LCCs residing in invaginations of the surface membrane called T-tubules (Figure 3A). Together with a host of other regulatory proteins, they form a Ca-signaling microdomain at each of these T-tubular membrane/SR membrane junctions. When one or more of the LCCs in the microdomain opens during an action potential, the Ca ions flowing into the narrow intermembrane space cause the nearby RyRs to open and release Ca ions stored within the SR into the cytoplasm, which can be imaged confocally as Ca sparks (Figure 3C). As the number of LCCs that open increases, more CRUs release their local store of SR Ca into the cytoplasm and the resulting Ca sparks summate together in a graded fashion to generate the whole cell CaT that determines the strength of contraction. Subsequently, the released Ca is pumped back into the SR by sarco-endoplasmic reticulum Ca ATPase (SERCA) pumps in the SR membrane or extruded into the extracellular space via the Na-Ca exchanger in the surface membrane.
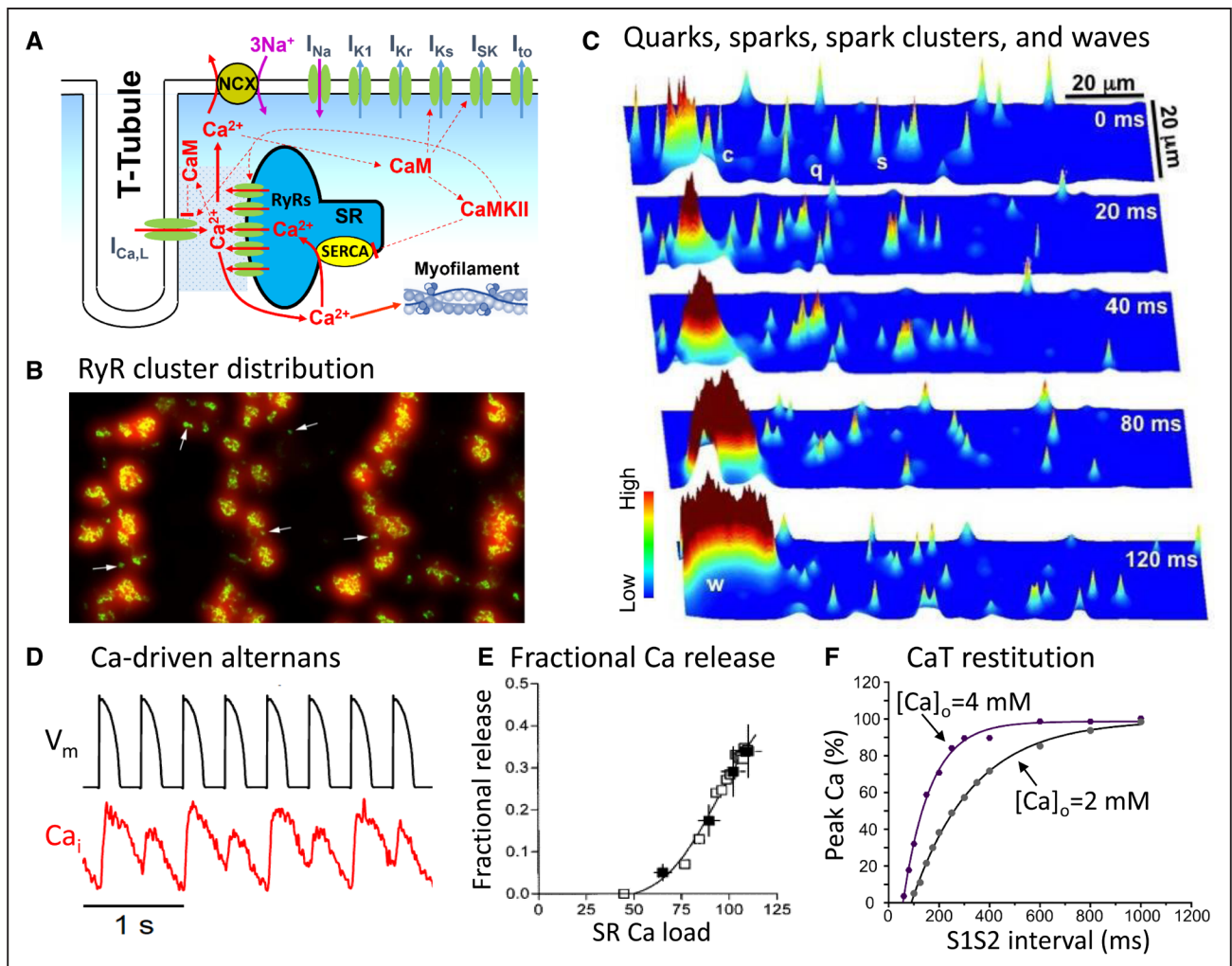
Figure 3. Cardiac Ca cycling.
A, Schematic diagram of a single calcium release unit (CRU) at a T-tubular membrane-sarcoplasmic reticulum (SR) membrane junction. **B**, A high-resolution image of the Ryanodine receptor (RyR) clusters in individual CRUs located in the T-tubule network of a rat ventricular myocyte.[62] **C**, Simulation demonstrating the Ca signaling hierarchy of quarks (q), sparks (s), and spark clusters (c) in a computer model of a ventricular myocyte.[66] In the time sequence illustrated, one of the clusters at the left eventually propagates as a mini-wave (w) by recruiting adjacent clusters. **D**, Primary Ca-driven alternans in a rabbit ventricular myocyte during pacing with a action potential (AP) clamp waveform.[67] **E**, The fractional SR Ca release curve measured in a rabbit ventricular myocyte.[69] **F**, Ca transient (CaT) restitution curves at 2 different extracellular [Ca]$_o$ recorded from mouse ventricular myocytes using the S1S2 extrastimulus method.[72] CaM indicates calmodulin; CaMKII, Ca/calmodulin-dependent protein kinase II; and NCX, Na-Ca exchange.

Several additional features of the CRU network play critical roles in the genesis of CaT alternans. The first feature is related to the fact that the CRUs in the network are coupled via Ca diffusion both inside the network SR and throughout the cytoplasm, such that the firing of a CRU affects and is affected by its neighbors. For example, when 1 CRU fires, the released Ca diffusing to the neighboring CRUs can cause their RyRs to open so that they too fire; that is, a firing CRU can sometimes recruit nearby CRUs to fire, a process called spark-induced sparks.[63] Therefore, besides individual sparks triggered directly by LCC openings, spark clusters (macrosparks) and spark-induced Ca waves can also occur via spark-induced sparks (Figure 3C).[64–66] In addition, as the SR Ca load increases, the greater amount of Ca released by

each spark increases the recruitment probability of additional spark-induced sparks. This causes the fraction of SR Ca released by the CRU network to increase steeply when the SR Ca load exceeds a certain level.[67,68] The relationship between the fraction of SR Ca released and SR Ca load can be measured experimentally[69] and quantified as the fractional SR Ca release curve (Figure 3E). The second key feature is that once a CRU fires and releases its local SR Ca store, there is a time delay before it becomes available to fire again, called Ca spark restitution.[70,71] It is this recovery period that underlies the CaT restitution curve shown in Figure 3F.[72] Since SR refilling is faster than RyR recovery,[70,73] the CaT restitution curve is mainly determined by RyR recovery kinetics, mediated by regions of the RyR protein that sense the intraluminal

SR Ca levels, either directly[74] or through interactions with intraluminal accessory SR proteins such as triadin, junction, and calsequestrin.[75] With this background, it is now possible to understand the 2 main mechanisms that cause CaT alternans[56,63,68,76–79] and how they synergize with each other at fast heart rates.[68]

CaT alternans driven by SR Ca load alternans

Based on experimental studies[59,60,80] demonstrating that CaT alternans could be elicited at heart rates too slow to encounter RyR refractoriness and CaT restitution, Eisner et al[76] proposed that a steep fractional SR Ca release curve could explain CaT alternans in the following manner. In the steep region of the fractional SR Ca release curve, a small change in SR Ca load results in a larger change in fractional SR Ca release (due to more spark-induced sparks), creating a positive feedback relationship. Thus, if slightly more SR Ca is released on the nth beat, the resulting CaT will be larger, but the SR Ca load becomes more depleted. If the SERCA pump is not capable of restoring all of the released Ca back into the SR, this will result in a smaller SR Ca load prior to the $(n+1)$th beat. This in turn causes a smaller fractional Ca release and CaT on that beat, such that more SR Ca will be available for release on the $(n+2)$th beat, resulting in a greater fractional SR Ca release and CaT, and so forth in an alternating fashion. This mechanism has been formulated mathematically using iterative map approaches,[10,56,68,77] and its prediction that CaT alternans is promoted by increasing the steepness of the fractional SR Ca release curve and decreasing the SR Ca reuptake rate via SERCA (Figure 4A) has been confirmed experimentally in isolated ventricular myocytes.[81] Since spark-induced spark recruitment enhances the steepness of fractional SR Ca release curve,[67,68] this mechanism is also consistent with the observation that Ca mini-waves occur during CaT alternans (Figure 4B). Relevant to heart disease, computer simulations show that T-tubule disruption, a feature of heart failure remodeling, steepens the fractional SR Ca release curve by reducing LCC-triggered CRU firings to allow more recruitments to occur, and thereby promotes SR Ca load alternans driving CaT alternans.[82]

CaT alternans driven by RyR refractoriness

In the CaT alternans mechanism above, it is obligatory for the SR Ca load to alternate concomitantly with the CaT, since the Ca release is uniquely determined by the SR Ca load. However, other experiments have shown that CaT alternans can occur without the SR Ca load alternating in the expected fashion,[83–85] indicating that another mechanism must also be at play. In experimental studies in both ventricular and atrial myocytes,[61,84–89] this other mechanism has been identified as RyR refractoriness, and explained by a complementary theory, called the 3R theory.[63,67] The "3R" refers to 3 fundamental phenomenological properties

of CRUs: *R*andom firings due stochastic LCC and RyR openings, *R*efractoriness requiring a recovery period for a CRU to regain excitability after firing, and *R*ecruitment of neighboring unactivated CRUs to fire and initiate a spark cluster or Ca wave. CaT alternans without SR load alternans can occur during pacing when, due to RyR refractoriness, some CRUs fire only on every other beat (or even randomly).[63,90] If the CRUs are not strongly coupled, their firings occur randomly out-of-phase, and thus the summation of sparks gives rise to a whole-cell CaT without macroscopic alternans. However, if the CRUs are strongly coupled such that spark-induced spark recruitment occurs, the firings from adjacent CRUs can become locally synchronized, forming firing clusters or mini-waves (Figure 4B). Due to this recruitment or synchronization effect, as more CRUs fire in 1 beat and less in the next beat, whole cell CaT begins to alternate macroscopically. In other words, if there is no coupling between CRUs or the coupling is weak, one can see alternans in individual CRUs but not in the global signal. Once the coupling is strong enough, however, the individual alternans become synchronized to produce global alternans. This was directly observed during experiments in rat ventricular myocytes by Tian et al[90] who showed that microscopic alternans (ie, alternans in individual CRUs) but not macroscopic alternans occurred at slower pacing rates, whereas both microscopic and macroscopic alternans occurred together at faster pacing rates as coupling and recruitment became stronger with increased SR Ca loading (Figure 4C). Under such conditions, computer simulations[63,79] have shown that alternans can occur even when SR Ca load is artificially clamped at a constant level. However, since the spark firing rate and recruitment depend on the SR Ca load, SR Ca load still plays an important role in this mechanism of alternans.[68,79] Similarly, although SERCA activity is not an apparent parameter in this theory, it also plays an important role by affecting CRU coupling and the SR Ca load.[79]

A unified theory of CaT alternans

In the 2 mechanisms of CaT alternans, one depends on encountering short DIs at which RyR are still partially refractory and the other does not. The refractoriness-dependent mechanism is promoted by fast heart rates, as necessary to encounter refractoriness, but the SR Ca load-dependent mechanism can occur at any heart rate as long as SR Ca loading conditions for alternans are met (Figure 4A). A unified theory has recently been developed that combines both mechanisms into the same theoretical framework.[68] This theory demonstrates that the 2 mechanisms can work in synergy to promote CaT alternans at fast heart rates encountering RyR refractoriness. Therefore, both mechanisms may be responsible for CaT alternans observed at fast heart rates.[84,88,91] At slow heart rates at which RyRs fully recover between beats, however,
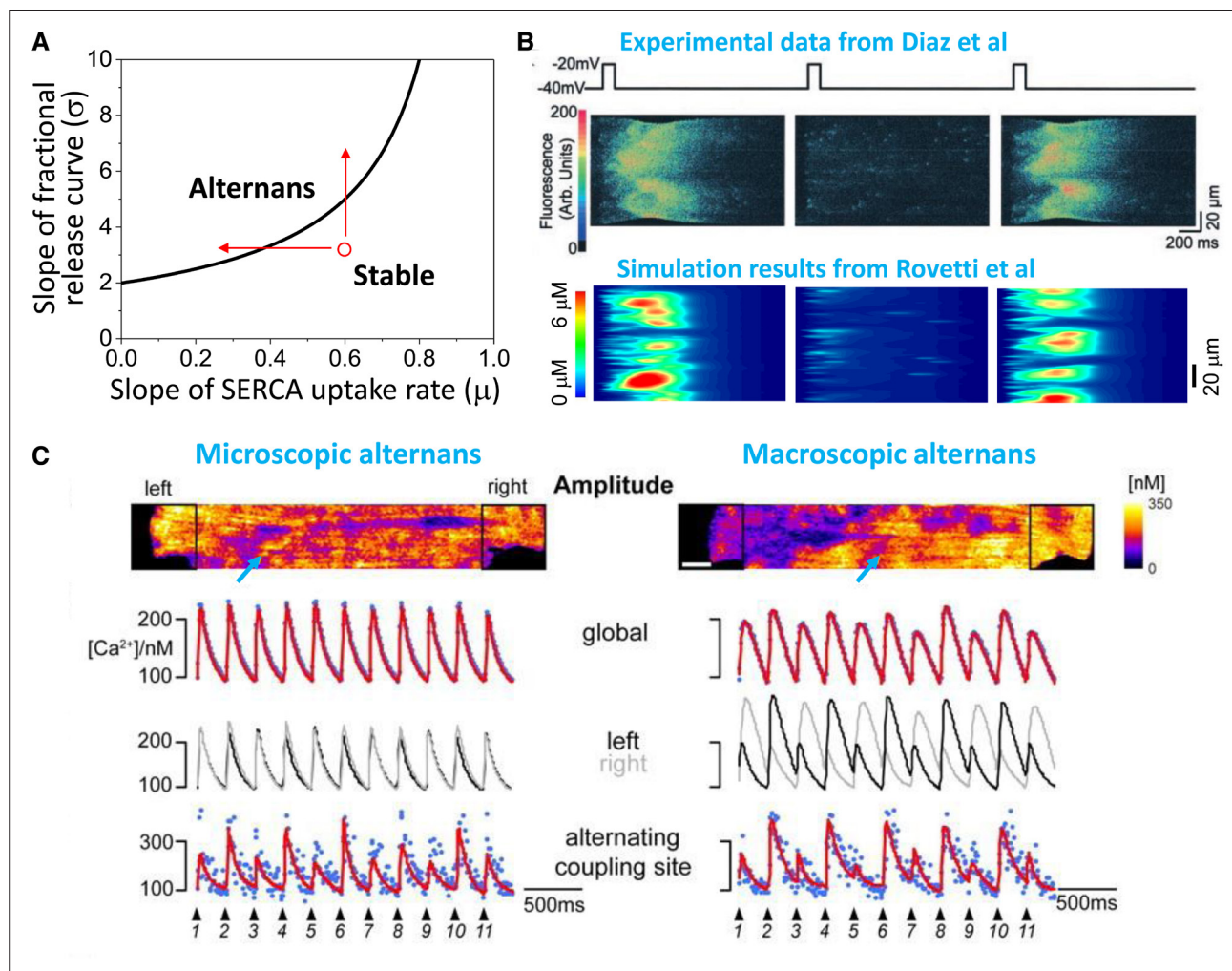
Figure 4. Mechanisms of Ca-driven alternans.
A, Calcium transient (CaT) alternans driven by sarcoplasmic reticulum (SR) Ca load alternans. Plot of the slopes of the fractional SR Ca release curve versus sarco-endoplasmic reticular Ca ATPase (SERCA) pump rate, in which the line indicates the region above which CaT alternans occurs. CaT alternans is promoted by either reducing the SERCA pump rate or increasing the steepness of the fractional SR Ca release curve (arrows). **B**, Confocal linescans of Ca fluorescence showing Ca mini-waves during alternans recorded in a rat ventricular myocyte[60] (top) and simulated in a computer model (bottom).[63] **C**, Transition from microscopic CaT alternans to macroscopic alternans as pacing frequency was increased in a rat ventricular myocyte.[90] **Left** column, Confocal image and traces at the slower pacing rate show microscopic alternans (lower trace) at the site (marked by arrow) in the confocal image above, in the absence of global macroscopic alternans (upper traces). **Right** column, At the faster pacing rate, both microscopic (lower trace) and macroscopic alternans (upper traces) are present. Moreover, the 2 ends of the myocyte (superimposed black and gray traces in the middle trace) are alternating out-of-phase, forming subcellular discordant alternans.

the SR Ca load-dependent alternans mechanism alone is responsible. Despite this difference, the 2 mechanisms are promoted by several common factors,[68,79] including disrupted T-tubules[82,92] and enhanced CRU coupling promoted by increased RyR sensitivity, reduced SERCA activity, reduced CRU spacing, and an appropriate SR Ca load. These factors promote recruitment to induce Ca mini-waves (Figure 4B) that play important roles in both mechanisms.[59,63,80,93] Among these factors, SERCA pump activity (which is highly regulated by catecholamines) is important to both mechanisms, supported by experiments that CaT alternans is promoted by SERCA reduction.[81,94–96] Most of the other common factors, such as T-tubule disruption,[97–99] reduced CRU spacing,[100] leaky

RyRs, and reduced SERCA activity are also promoted by heart failure remodeling.

Subcellular discordant CaT alternans
The pattern of CaT alternans within a myocyte can become out-of-phase spatially, such that during the same beat, CaT alternates high-low in 1 region but low-high in an adjacent region. This so-called subcellular discordant CaT alternans (Figure 4C, trace labeled left/right) has been well documented in experimental studies.[59,101–104] Theoretical analyses combined with simulations[92,105,106] have shown that when Ca-to-APD coupling is negative (see next section), subcellular CaT alternans can occur whether the heart is paced with either a free-running action potential or a constant voltage-clamped

waveform. Subcellular discordant CaT alternans does not occur when Ca-to-APD coupling is positive unless SR Ca release properties are heterogeneous[103] or the cell is paced with a constant voltage-clamped waveform.[106] Subcellular discordant CaT alternans is also promoted by T-tubule disruption or in cells with sparse T-tubule structures.[92] When subcellular discordant alternans occurs, the beat-to-beat differences in whole-cell CaT amplitude are reduced (or even eliminated if exactly half of the myocyte is out-of-phase with the other half). The amplitude of APD alternans is also reduced, commensurate with the reduced amplitude of the whole-cell CaT alternans.

Coupling of Voltage and Ca

As noted previously, voltage and Ca are bidirectionally coupled via Ca-dependent ionic currents/transporters as well as by Ca-dependent signaling (Figure 3A). For example, a large CaT increases inward Na-Ca exchange current, tending to prolong APD, but also accelerates LCC inactivation and increases both the slow component of the delayed rectifier K current and the Ca-activated small conductance K current,[107,108] tending to shorten APD. If the net effect is to enhance inward current during the action potential plateau, the Ca-to-APD coupling relationship is said to be positive, such that increasing the CaT amplitude prolongs APD. Thus, during alternans, the larger CaT corresponds to the longer APD, referred to as electromechanically concordant alternans (Figure 5A).[109] If the net effect is to enhance outward current during the action potential plateau, Ca-to-APD coupling is said to be negative, such that increasing CaT amplitude shortens APD. In this case, during alternans the larger CaT corresponds to the shorter APD, referred to as electromechanically discordant alternans (Figure 5B).

Conversely, APD also directly influences the CaT. By favoring SR Ca reuptake over Ca extrusion via electrogenic Na-Ca exchange current, a longer APD tends to increase SR Ca loading and augment the subsequent CaT. However, at constant heart rate, a longer APD also results in a shorter DI, which can impinge on the recovery of LCCs and RyRs available to release SR Ca on the next beat, thereby reducing the subsequent CaT. Thus, lengthening APD in the present beat can either enhance Ca release or reduce Ca release on the following beat, causing APD-to-Ca coupling to be positive or negative. Generally, during steep APDR slope-induced alternans, APD-to-Ca coupling is positive, but negative coupling can occur at slow heart rates due to SR Ca loading effects.[106] During early repolarization-induced alternans, APD-to-Ca coupling is also positive, since early repolarization truncates Ca entry and release during the very short action potential, after which the long DI allows full recovery of LCC and RyR excitability. For EAD-induced alternans, however, APD-to-Ca coupling tends to be negative, since the prolongation of APD by

EADs increases the SR Ca load available for release on the subsequent beat with the shorter APD.

Theoretical analysis[56,110] shows that when Ca-to-APD and APD-to-Ca coupling are both positive, the voltage-driven and Ca-driven instabilities work synergistically to cause the system to become more unstable (ie, more prone to alternans; Figure 5C). Conversely, when the Ca-to-APD coupling and APD-to-Ca coupling have opposite signs, the antagonism makes the system more stable (ie, less prone to alternans; Figure 5D), but eventually exhibits either electromechanically concordant or discordant alternans depending on which instability predominates. If the instabilities of the Ca subsystem and voltage subsystem are evenly balanced, however, a new behavior emerges in which the APD and CaT alternans oscillates quasiperiodically (the EMQA region in Figure 5D). Although direct experimental demonstration of the quasiperiodic behavior is not available, the quasiperiodic APD alternans caused by infusion of erythromycin in guinea pig hearts (Figure 5E)[111] can potentially be explained by this mechanism.

TISSUE-SCALE MANIFESTATIONS OF ALTERNANS

So far, we have outlined the features of alternans at the cellular scale. We now turn to the tissue scale in which adjacent myocytes are coupled via gap junctions allowing voltage but not intracellular Ca to diffuse efficiently from myocyte-to-myocyte.

Spatially Discordant Alternans

APD alternans that is uniformly in-phase throughout the whole tissue is called *spatially concordant* alternans (Figure 6A) (not to be confused with electromechanically concordant alternans). However, APD alternans can also become out-of-phase in different regions of the tissue, called *spatially discordant* alternans (SDA) (Figure 6B).[112–114] In this case, the out-of-phase regions are separated by a nodal line in which APD is constant from beat to beat. SDA is a highly arrhythmogenic situation because it generates marked dispersion of refractoriness that can result in unidirectional conduction block and initiation of reentry when the tissue APD gradient across the border of the discordant regions reaches a critical steepness, as discussed in detail later.

Several mechanisms have been shown to cause SDA. Conduction velocity restitution (CVR) is 1 key mechanism.[114,115] Analogous to APDR, the CVR curve quantifies the decrease in conduction velocity as the DI shortens due to incomplete recovery of the Na current. In this experimentally well-supported mechanism,[116–120] the onset of SDA occurs at heart rates which encounter CVR
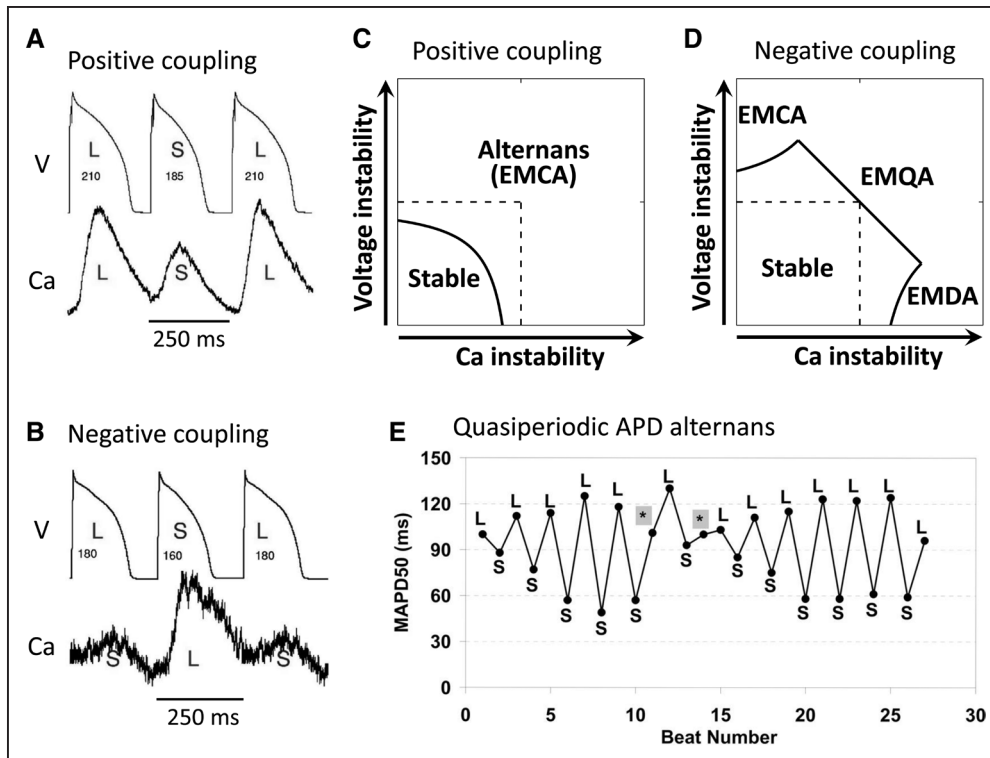
Figure 5. Effects of voltage and Ca coupling on alternans dynamics.
A–**D**, Action potential duration (APD)-to-Ca coupling is assumed to be positive and labels refer to Ca-to-APD coupling sign. **A**, Electromechanically concordant alternans (EMCA) in a rabbit ventricular myocyte with positive Ca-to-APD coupling.[109] **B**, Electromechanically discordant alternans (EMDA) in a rabbit myocyte after blocking Na-Ca exchange current by SEA0400 to promote negative Ca-to-APD coupling.[109] **C**, Theoretical stability boundary of alternans for positive Ca-to-APD coupling.[123] Arrows along both axes indicate the directions of increasing instability and dashed lines are the stability boundaries (from stable to unstable) when Ca and APD are not coupled. Solid line is the stability boundary when Ca and APD are coupled, below which the system is stable without alternans and above which alternans occurs in the form of EMCA. **D**, Same as C but for negative Ca-to-APD coupling. The regions of EMCA, EMDA, and electromechanically quasiperiodic alternans (EMQA) are marked. **E**, Quasiperiodic APD alternans caused by infusion of erythromycin in guinea pig hearts.[111]

(ie, in which the DI is short enough to slow conduction velocity due to CVR), which typically occurs at fast heart rates. However, other experimental[120–122] as well as simulation and theoretical studies[32,123] have shown that SDA can also be induced by premature ventricular extrasystoles (PVC) and tissue heterogeneities without encountering CVR. Since encountering CVR is not required, these latter mechanisms can produce SDA at normal or even slow heart rates.

Regional alternans can also result in SDA-like patterns, when alternans amplitude varies significantly from 1 region to another, thereby generating dispersion of repolarization. An extreme case is regional 2:1 block due to APD dispersion or weak excitability.

Unlike rapid diffusion of voltage from cell-to-cell through gap junctions, intercellular Ca diffusion is slow and limited[124] such that the CaT can alternate out-of-phase in neighboring cells. However, if CaT alternans is out-of-phase over small spatial scales, the APD differences will be smoothed by voltage diffusion and diminished (Figure 6C, right). Only if CaT alternans is synchronized over large spatial clusters can a large APD gradient form in response (Figure 6C, left). Recent theoretical analysis[123]

has shown that maintained synchronization is promoted by large initially synchronized spatial Ca SDA clusters or when the APD-to-Ca coupling is strong. When APD and CaT alternans are dyssynchronous, their nodal lines may or may not co-localize with each other in tissue, as also noted in experiments.[36,116,121,122]

Regional Chaos Synchronization Causing T-Wave Lability

Unlike SDA generated by either CVR or pre-existing repolarization heterogeneities, when APD alternans transitions into chaotic APD behavior (Figure 2), voltage diffusion will cause tissue APD to spontaneously synchronize regionally, but not globally, such that the regional APD distribution varies chaotically from beat to beat.[44] This will cause the repolarization sequence and hence the T-wave morphology to vary irregularly from beat to beat, resulting in T-wave lability (Figure 6D).[47] The underlying marked dispersion of repolarization creates a highly arrhythmogenic tissue substrate susceptible to initiation of reentry by not only exogenous PVCs, but also by self-generated PVCs, as described in the next section.
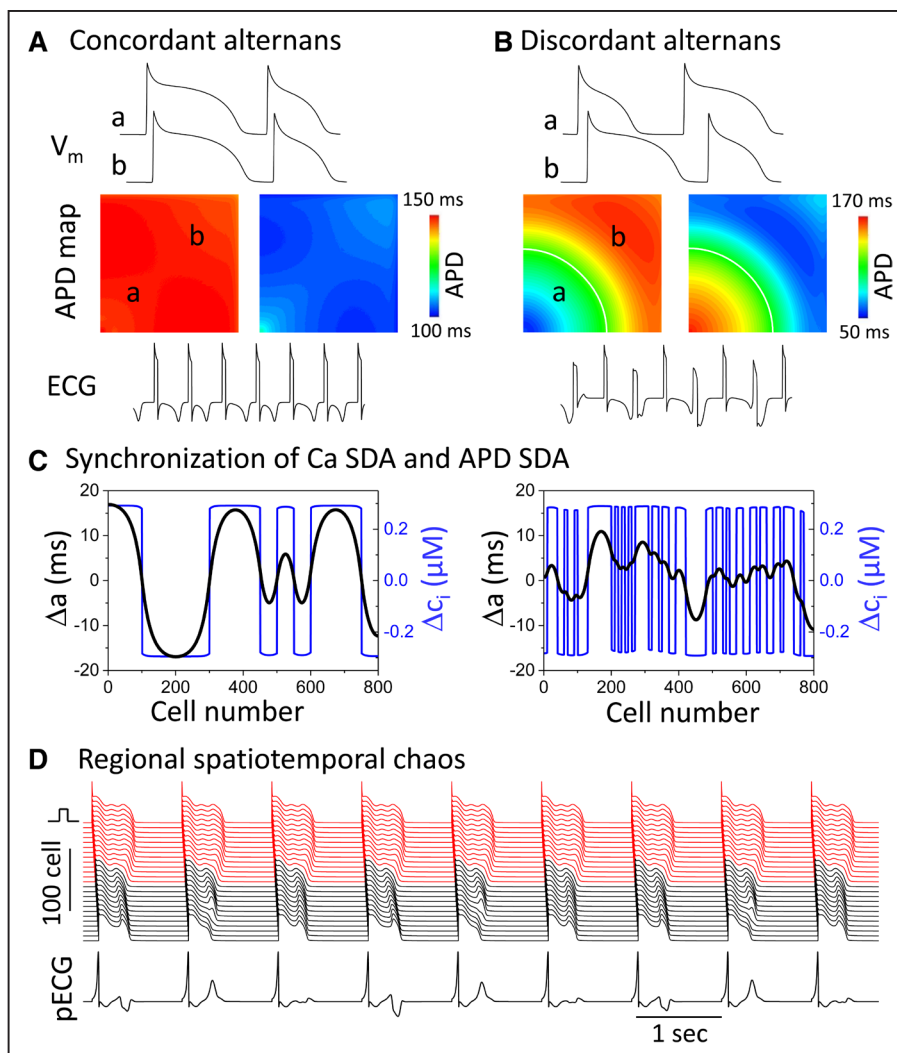
Figure 6. Spatially discordant alternans (SDA) and regional spatiotemporal chaos in cardiac tissue.
A, At a critical heart rate, action potential duration (APD) begins to alternate concordantly in a long-short pattern over the entire simulated 2-dimensional homogeneous tissue (spatially concordant alternans). During either the long or short APD beat, the APD gradient is minimal, but the QT interval alternates in the simulated electrocardiogram (ECG) tracing below. **B**, As heart rate increases sufficiently to encounter conduction velocity restitution (CVR), APD alternans becomes spatially discordant, exhibiting a short-long pattern in region *a* and a long-short pattern in region *b*, separated by a nodal line without alternans (white line). The result is a marked APD gradient which reverses on alternating beats, causing both T-wave alternans (TWA) and QRS alternans (QRSA) in the simulated ECG tracing below. **C**, Attenuation of the amplitude of APD alternans (Δa) by spatially dyssynchronous calcium transient (CaT) alternans (Δc_i) in a simulated 1-dimensional cable of rabbit ventricular myocytes. APD alternans amplitude is greater when CaT alternans is synchronized in large clusters of adjacent myocytes (left) compared with a more random spatial distribution (right).[123] **D**, Regional spatiotemporal chaos in a simulated 1-dimensional cable containing a long APD region at the top (red) next to a region with chaotic early afterdepolarizations (EAD) at the bottom (black).[47] The APD variation in the chaotic region causes the repolarization sequence to vary from beat to beat such that the T-wave amplitude, shape and polarity changes chaotically from beat to beat, causing marked T-wave lability, even though the QT interval (determined primarily by the long APD region) remains unchanged.

ALTERNANS AND ARRHYTHMOGENESIS

We previously classified ventricular arrhythmias into 3 dynamics-based categories[30]: Ca cycling disorders, prolonged repolarization disorders, and early repolarization disorders. As discussed above, cardiac alternans is a common feature of all 3, and, in the form of SDA or regional chaos synchronization, results in marked dispersion of repolarization, creating a tissue substrate highly vulnerable to reentry. In this setting, a PVC arising from a different location or an exogenous source that propagates into a region with a steep APD gradient can block locally, resulting in 2 wavefronts that propagate around the long APD region to form a figure-of-eight reentry, classically known as the R-on-T phenomenon (Figure 7A and 7B). Moreover, simulations and experiments also indicate the APD gradient can itself spontaneously generate a PVC during its repolarization process that then propagates around the long APD region to initiate reentry (Figure 7C).[125,126] To distinguish between these 2 variations of the R-on-T phenomenon, we refer to the exogenous

PVC case as the R-to-T mechanism, and the self-generated PVC case as the R-from-T mechanism. Here we review the conditions under which cardiac alternans leads to initiation of reentrant arrhythmias via these 2 mechanisms. The important conclusion is that cardiac alternans represents more than just an early sign of electrical instability in cardiac tissue, but also serves as a self-contained causal mechanism initiating lethal reentrant ventricular arrhythmias. Although less thoroughly characterized, these findings are also highly relevant to atrial arrhythmias, as discussed in this section later.

Ca Cycling Disorders

The purest example of an arrhythmogenic Ca cycling disorder is CPVT typically caused by ryanodine and calsequestrin mutations.[127,128] However, disordered Ca cycling is also a prominent feature of heart failure, chronic and acute ischemia, digitalis toxicity and other Ca overload conditions, as well as normal hearts subjected to very rapid heart rates. In normal mammalian heart, experimental studies[36–39,129] have shown that alternans occurs well before APDR slope becomes >1, indicating that Ca-driven alternans predominates in setting the heart rate
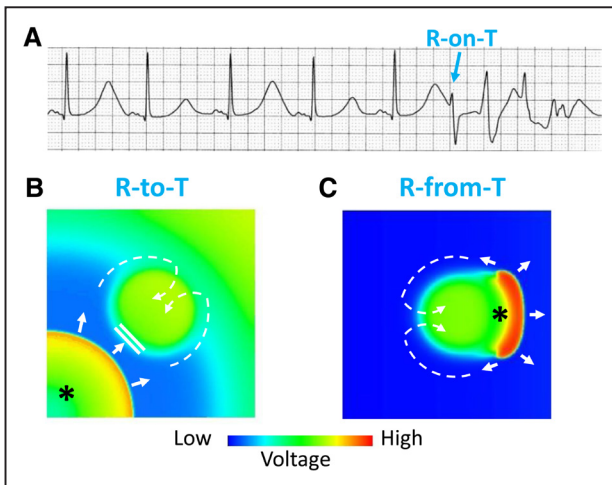

Figure 7. R-to-T and R-from-T mechanisms linking T-wave alternans (TWA) to arrhythmogenesis.
A, Electrocardiogram showing TWA and an R-on-T event (*) initiating Torsade de pointes . **B**, Voltage snapshot illustrating the "R-to-T" mechanism in which a premature ventricular complex (PVC) (*) emerging from a separate location (lower corner) propagates towards a central prolonged action potential duration (APD) region that is still repolarizing, where it blocks locally and then proceeds around and reenters the blocked region after it has repolarized (dashed arrows), thereby initiating figure-of-eight reentry. **C**, Voltage snapshot showing the "R-from-T" mechanism in which the PVC (*) is generated directly by electronic current flow from the central region with delayed repolarization into already repolarized tissue. The PVC then conducts around and reenter the heterogeneous region to initiate figure-of-eight reentry (dashed arrows). This requires the central region to have a longer APD (eg, due to an early afterdepolarization [EAD] or action potential [AP] dome) which repolarizes much later than surrounding tissue (eg, without an EAD or AP dome).

threshold for the onset of TWA in normal human heart. However, since voltage and Ca are coupled, the APDR slope (even if <1) also contributes to either promoting or suppressing the threshold heart rate for the onset of TWA, depending on whether Ca-to-APD and APD-to-Ca coupling have the same or opposite signs (see Figure 5C).

As pacing rate accelerates, spatially concordant APD and CaT alternans develop first, but this does not markedly increase APD dispersion, since on each beat, APD is either uniformly long or uniformly short (Figure 6A). However, reentry can be initiated when loss of 1:1 capture occurs or a properly-timed PVC occurs, assuming some pre-existing APD dispersion is present.

With further increases in heart rate sufficient to encounter CVR, spatially concordant alternans transitions to SDA in which APD dispersion markedly increases (Figure 6B). In this setting, a PVC emerging from the short APD region can block locally as it attempts to propagate across the nodal line where the APD gradient is steepest, proceed laterally to circumvent the line of conduction block and then reenter the long APD region after it recovers excitability to initiate reentry. However, since all real cardiac tissue is inherently heterogeneous, such that APD alternans amplitude is larger in some regions than others, an exogenous PVC may not be required. Instead, a paced beat can develop localized conduction block in the region where the APD gradient is steepest during SDA. In this setting, SDA alone, without a PVC arising from an independent source, is causally sufficient to induce reentry. The same mechanisms apply to transient SDA induced by a PVC or regional tissue heterogeneity at DIs not short enough to encounter CVR.

In normal ventricles, the initiation of lethal arrhythmias by the SDA mechanism requires nonphysiologically rapid heart rates, generally >250–300 bpm in human hearts. However, disease conditions that impair Ca cycling at physiological heart rates, such as CPVT, heart failure, acute and chronic ischemia, digitalis toxicity, can cause the same lethal arrhythmias to occur at much slower heart rates. Moreover, when Ca cycling is impaired, ventricular tissue not only becomes predisposed to Ca-driven alternans and SDA, but also to delayed afterdepolarizations (DAD) and triggered activity caused by spontaneous diastolic SR Ca release. Thus, even if SDA creates a vulnerable substrate that does not generate unidirectional conduction block and initiate reentry on its own, Ca cycling disorders also endogenously generate DAD-mediated PVC triggers as well as dispersion of excitability that can promote reentry initiation.[130]

Prolonged Repolarization Disorders

The purest examples of arrhythmogenic prolonged repolarization disorders are inherited or drug-induced LQTS. Prolonged repolarization is also a feature of heart failure

and chronic ischemic heart disease in which electrical modeling reduces repolarization reserve. TWA, in this setting, is mainly voltage-driven by EAD-induced alternans, which occurs when heart rate slows sufficiently to allow EADs to emerge on every other beat, as illustrated in Figure 2B. Within the span of heart rates causing alternans, however, there are typically also windows in which higher order periodicities and frankly chaotic behavior emerge. In these chaotic windows, regional chaos synchronization[47] causes the heart tissue to form regions with prolonged APD due to EADs next to regions with shorter APD without EADs, resulting in marked regional APD dispersion. Therefore, in this setting, large APD gradients can result from regional alternans,[47] non-CVR-mediated SDA,[32] or regional chaos synchronization.[44] Not only is the resulting substrate vulnerable to initiation of reentrant arrhythmias by an exogenous PVC, but the substrate can also directly generate a PVC to initiate reentry at a distant site by the R-to-T mechanism (Figure 7B), or locally at the same site by the R-from-T mechanism (Figure 7C).[47,125,126] Electrocardiographically, the chaotic shifting of the EAD regions on each beat when regional chaos synchronization occurs causes the T-wave morphology to vary from beat to beat, resulting in T-wave lability (Figure 6D).

As mentioned earlier, APD alternans can also occur at normal or slow heart rates via the steep APDR slope-driven mechanism when no EADs are present, as long as APD is sufficiently prolonged (eg, left in Figure 2A). In this case, regional alternans or CVR-mediated SDA can generate steep enough APD gradients in LQTS to initiate reentry via either of the 2 mechanisms in Figure 7.

Early Repolarization Disorders

The purest examples of arrhythmogenic early repolarization disorders are Brugada syndrome and short QT syndromes.[131] However, early repolarization is also a feature of acute myocardial ischemia in which activation of ATP-sensitive K channels and other metabolic sequelae enhance repolarization reserve.[49] In these settings, TWA is mainly voltage-driven by early repolarization-induced alternans, occurring at heart rates in which all-or-none early repolarization occurs on every other beat (Figure 2C). As in LQTS, however, within the span of heart rates causing alternans are windows in which higher order periodicities and frankly chaotic behavior emerge. In these chaotic windows, regional chaos synchronization[47] can cause the heart tissue to form early repolarizing regions with very short spike-only action potentials next to regions with normal spike-and-dome action potentials, resulting in marked tissue APD dispersion. Thus, 3 separate mechanisms can cause large APD gradients in this setting: regional chaos synchronization,[44] regional variation in alternans amplitude,[47] and non-CVR-mediated

SDA.[32] The resulting marked APD dispersion makes the tissue susceptible to initiation of reentry by an exogenous PVC via the R-to-T mechanism (Figure 7B). However, the steep repolarization gradient can also self-generate a PVC, due to electronic current flow between a still-depolarized spike-and-dome action potential region and an adjacent spike-only action potential region that has repolarized early and can be reexcited. This reexcitation results in so-called phase-2 reentry[132] via the R-from-T mechanism, as illustrated in Figure 7C. In Brugada syndrome, TWA has been widely observed[133–136] and often occurs simultaneously with PVCs,[133,136] consistent with the R-from-T mechanism. However, the role of early repolarization and phase-2 reentry in Brugada syndrome (the so-called repolarization hypothesis) is currently controversial. Some investigators favor an alternative depolarization hypothesis that structural changes due to fibrosis in regions of the right ventricular epicardium cause slow conduction predisposing these patients to reentry initiation.[137,138] The 2 hypotheses are not necessarily mutually exclusive, however, and could be synergistic or even causally related.[139] Overall, the role of TWA as a predictor of serious arrhythmia events in Brugada syndrome remains controversial.[134,135]

Atrial Arrhythmias

Atrial repolarization alternans, including SDA, has been detected during sinus rhythm or rapid pacing immediately prior to the onset of atrial fibrillation (AF) in both humans[38,140,141] and animal experiments.[142–145] The mechanisms of APD and CaT alternans have been analyzed in experimental and simulation studies of both isolated atrial myocytes and atrial tissue,[61,83,85,89,145–149] with most of these studies suggesting that the onset of alternans is primarily Ca-driven due to the RyR refractoriness mechanism.[85,89,148] For example, in a clinical study by Narayan et al,[38] patients with a history of persistent AF typically developed APD alternans during atrial pacing at near-normal heart rates at which APDR slope was <1, pointing to Ca-driven alternans related to AF-induced Ca cycling remodeling as the predominant initiating mechanism. In contrast, control patients required faster pacing rates to develop APD alternans, but its onset still bore no consistent relationship to APDR slope being >1 or <1. This agrees with the observation by Pearman et al[147] in sheep atria that APD and CaT alternans at slow heart rates were abolished when SR Ca cycling was disabled by thapsigargin treatment, but not at faster heart rates at which ADPR slope was steeper. A recent comprehensive study in perfused canine atria by Liu et al[89] came to similar conclusions, and also documented with optical mapping that wavebreak causing AF initiation occurred after the transition from spatially concordant alternans to SDA as pacing rate increased, as had previously

been observed in humans.[141] CaT alternans in atrial tissue is likely to be facilitated by the sparse T-tubular network in atrial myocytes,[150–152] which steepens the CaT restitution curve by facilitating spark-induced spark recruitment.[82,92] To summarize, both voltage-driven and Ca-driven mechanisms of alternans are important in atrial tissue. The coupling between voltage and Ca implies that even when the APDR slope is <1, voltage-driven mechanisms are contributing to either promoting or suppressing the onset of TWA by Ca-driven mechanisms, depending on whether Ca-to-APD and APD-to-Ca coupling have the same or opposite signs (see Figure 5C).

Other voltage-driven alternans mechanisms may also play a role in atrial arrhythmogenesis, including AF. Since EADs have been shown to occur in atrial myocytes,[153,154] in principle, EAD-induced alternans and regional chaos synchronization initiating reentry by mechanisms equivalent to R-from-T or R-to-T could also occur in atria. In aged rats, for example, mild glycolytic inhibition induced EADs alternans followed by rapid EAD-mediated triggered activity in the pulmonary veins that initiated AF (see Figure 5 in Ono et al[155]). In this case, rapid triggered activity from the pulmonary veins was most likely fast enough to induce SDA in the body of the atria which resulted in wavebreak initiating AF. Whether regional chaos synchronization played any role is unclear.

Whether the early repolarization alternans mechanism can cause atrial alternans and regional chaos synchronization to initiate AF is currently unclear. Due to its large I_{to} conductance, the atrial action potential is typically spike-like without a prominent action potential dome. Rapid atrial pacing, however, is well known to induce electrical remodeling that downregulates I_{to}. It is intriguing to speculate if I_{to} downregulation was sufficient to allow an action potential dome to reemerge intermittently in atrial myocytes, then the early repolarization alternans mechanism, as well as regional chaos synchronization and phase-2 reentry, could come into play. As yet, however, there is no experimental evidence directly supporting this conjecture.

Focal Arrhythmias and Anatomic Reentry

Cardiac alternans plays less of a direct mechanistic role in focal arrhythmias, with the possible exception of bidirectional VT seen in Ca cycling disorders like CPVT and digitalis toxicity. A mechanism for bidirectional VT proposed from simulations is DAD alternans, in which alternating sites of DAD-mediated triggered activity in the different branches of the His-Purkinje system or regions of ventricular myocardium trigger each other reciprocally in a ping-pong fashion such that the QRS morphology alternates, with secondary TWA changes due to the altered repolarization sequence.[156] If the rate of

bidirectional VT is fast enough to induce SDA, however, the resulting wavebreaks can cause degeneration into ventricular fibrillation, just like rapid-pacing induced VT or ventricular fibrillation.

For anatomic VT due to reentry around an anatomic obstacle, as occurs in scar-related VT and bundle branch macro-reentry, TWA and QRSA are also less important. However, transient cycle length alternans, related to CVR in slowly-conducting regions of the reentry circuit, is commonly observed, especially during initiation and termination of reentry. Transient cycle length alternans is also commonly observed in supraventricular arrhythmias involving anatomic reentry, including atrio-ventricular nodal reentry, and atrio-ventricular reentry using an accessory pathway(s).

BACK TO THE BEDSIDE

Electrocardiogram Signatures of Alternans

The electrocardiogram represents a weighted average of the voltage differences within the heart during the cardiac cycle, with the amplitude, shape, polarity and duration of various electrocardiogram components reflecting the underlying timing, direction and synchronicity of propagating depolarization/repolarization waves. Here we discuss the links between the cellular/tissue-scale mechanisms of alternans and their corresponding electrocardiogram patterns. For this purpose, we equate the QT and TQ (time interval between the T-wave and the next Q-wave) intervals (see Figure 8A) with average estimates of tissue APD and DI, respectively. Thus, during alternans at a constant heart rate, just as APD and DI alternate oppositely (i.e. long-short and short-long, respectively) such that pacing cycle length(=APD+DI) remains constant for each beat, the QT and TQ intervals also alternate oppositely such that RR = QT+TQ for each beat.

In simulated homogeneous tissue in which spatially concordant APD alternans is present with constant conduction velocity, the spatial repolarization sequence will match the depolarization sequence such that the amplitude, shape, and polarity of both the QRS and T-wave will be nearly identical for both long and short QT beats (Figure 6A). However, when the TQ interval (surrogate for DI) becomes short enough to encounter CVR and cause SDA, the changing conduction velocity of the depolarization wave as it propagates through the tissue will reverse on alternate beats, causing QRSA (Figure 6B).[113,114] Likewise, the out-of-phase alternating APD regions will increase the dispersion of repolarization and cause its spatial sequence to reverse on alternate beats, such that the T-wave widens and reverses polarity on alternate beats even in initially homogeneous tissue.

In real heart tissue, however, regional APD heterogeneity exists even in normal ventricles due to transmural
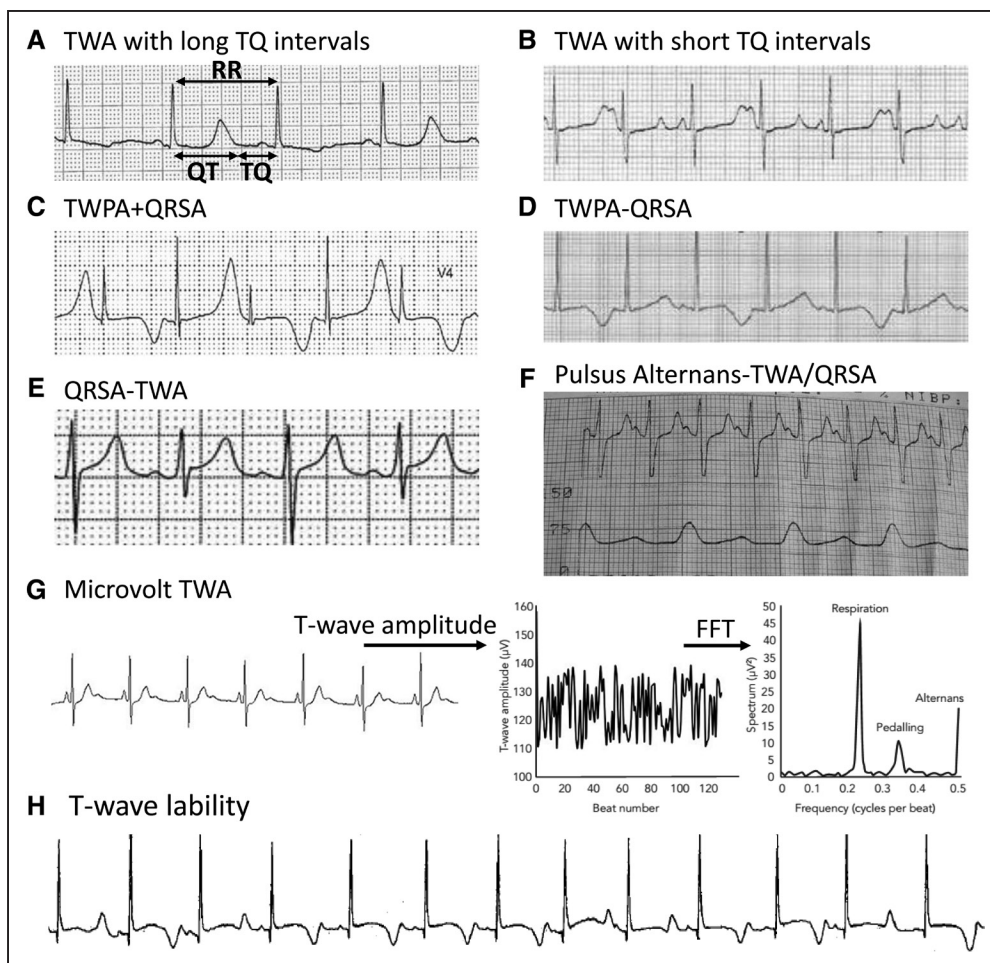
Figure 8. Clinical examples of alternans on recorded electrocardiograms.
A, T-wave alternans (TWA) with long TQ (time interval between the T-wave and the next Q-wave) intervals in a 52-year-old man with amiodarone-induced long QT syndrome (LQTS).[24] RR=QT+TQ. **B**, TWA with short TQ intervals from a 13-month-old girl with congenital LQTS.[157] **C**, TWA with T-wave polarity alternans (TWPA) and QRS complex (QRSA).[158] **D**, TWA with TWPA without QRSA in a 59-year old man with LQTS.[163] **E**, QRSA without TWA. **F**, Pulsus alternans without TWA.[168] **G**, Microvolt TWA detected using frequency-domain analysis (right).[170] **H**, A 1 year-old girl with Jervell-Lange-Nielson syndrome with multiple episodes of T-wave lability and Torsade de Pointes, who later died suddenly at 2 years of age.[171] FFT indicates fast fourier transform.

and base-to-apex APD gradients, and is often exacerbated by heart diseases. As a result, the spatial repolarization sequence and hence the T-wave amplitude, shape, and polarity often change on alternate beats, even during spatially concordant alternans. During SDA, however, the alternans in T-wave amplitude, shape, and especially its polarity becomes even more prominent. If SDA results from encountering CVR at short TQ intervals, then the QRS also alternates. If the TQ intervals are too long to encounter CVR and QRSA is therefore absent, then some other mechanism must be operative for SDA to occur. In principle, CaT alternans due to alternating SR Ca load can produce TWA at long TQ intervals. However, when alternans is Ca-driven, the TWA amplitude may not be as prominent if Ca-to-APD coupling is weak or if CaT alternans is spatially dyssynchronous.

Illustrative electrocardiogram traces from real patients are shown in Figure 8.

TWA with and without QRSA

In Figure 8A, the electrocardiogram trace from a patient with amiodarone-induced LQTS illustrates TWA with 2 relatively long alternating TQ intervals.[24] These long TQ intervals could plausibly correspond to DIs positioned on either side of the discontinuous steep region at which EADs suddenly prolong the APD in the APDR curve, as in Figure 2B, causing the QT intervals to alternate by the EAD-induced alternans mechanism. Note that in this tracing, both TQ intervals are too long to encounter CVR and cause SDA, as evidenced by the absence of QRSA. The alternans in T-wave amplitude, shape, and polarity are nevertheless prominent, however, and could potentially indicate underlying SDA due to a mechanism other than encountering CVR.

Figure 8B shows another electrocardiogram tracing from a congenital LQTS patient,[157] in which one of the alternating TQ intervals is potentially short enough to encounter CVR. TQ alternans is also accompanied by

REVIEW

prominent alternans in the T-wave amplitude and shape. However, QRSA is not present, indicating that if SDA is present, it is not related to encountering CVR.

Figure 8C, also obtained from an LQTS patient,[158] illustrates TWA with short TQ intervals and prominent T-wave polarity alternans, which is widely observed in LQTS.[19,22,159–162] Moreover, QRSA is also present, indicating a high probability of SDA due to encountering CVR at the short TQ intervals. The mechanism of alternans could be EAD-induced alternans (Figure 2B), but steep APDR slope-induced alternans (Figure 2A) or Ca-driven alternans (Figure 5) are also plausible in view of the short preceding TQ intervals. T-wave polarity alternans is also observed in LQTS patients with long TQ intervals and no QRSA (Figure 8D),[159,163] indicating that a non-CVR mechanism of SDA or regional alternans may be responsible. In Holter recordings, macroscopic T-wave polarity alternans episodes have been observed in up to 45% of congenital LQTS,[164] and often precede, sometimes immediately, episodes of Torsade de pointes, as illustrated in Figure 1B.

Early repolarization-mediated alternans in patients with early repolarization syndromes can also exhibit TWA with normal-to-long TQ intervals corresponding to the DIs at which all-or-none early repolarization suddenly occurs, as illustrated in the APDR curve in Figure 2C.

In CPVT and failing human hearts with disordered Ca cycling, Ca-driven alternans, rather than steep APDR slope voltage-driven alternans, is likely to be the mechanism initiating TWA, manifested initially as spatially concordant alternans with pulsus paradoxus. As heart rate increases and TQ intervals become short enough to encounter CVR, alternans transitions to SDA with QRSA. This is also true for normal human heart when paced nonphysiologically at very rapid rates (>250–300 bpm). Animal studies have confirmed that SDA in this setting is one of the key mechanisms by which very rapid pacing initiates reentrant polymorphic VT and ventricular fibrillation in normal hearts.[112,113]

Other causes of QRSA, with and without secondary TWA

QRSA, usually with secondary T-wave changes, can also occur in other conditions, such as bidirectional VT seen in Ca cycling disorders like CPVT and digitalis toxicity, and has been hypothesized to arise from DAD alternans.[156] Bundle branch block alternans is another form of QRSA sometimes observed in patients with conduction system disease, attributed to complex patterns of conduction block.[165] QRSA can also be observed with large pericardial effusions, thought to be related to pendulous motion of the heart swinging in the fluid-filled pericardial sack.[166] Finally, QRSA can occur without visible TWA (Figure 8E), although whether subtle microvolt TWA is present has not been excluded (see below).

Pulsus alternans without TWA

Pulsus alternans usually occurs with TWA or QRSA.[157,167] If alternans is Ca-driven and Ca-to-APD coupling is very weak, pulsus alternans can occur without discernible visible TWA[168,169] (Figure 8F).

Microvolt TWA

Microvolt TWA is a subtle form of repolarization alternans characterized by microvolt changes in T-wave amplitude that are not visible to the naked eye, but can be revealed by signal processing using either frequency-domain or time-domain techniques when heart rate is mildly elevated to 90–110 bpm (Figure 8G).[29,170] The exact mechanism underlying microvolt TWA is unknown, but 1 possibility is subtle Ca-driven alternans with weak Ca-to-APD coupling. In this case, mechanical pulsus alternans might be discernible without visibly appreciable TWA on electrocardiogram. Alternatively, even if Ca-to-APD coupling is strong, when CaT alternans is spatially dyssynchronous within or between adjacent myocytes, the alternans in voltage may be attenuated (see Figure 6C), and pulsus alternans also weak or absent. Another possibility is APD alternans or 2:1 conduction block in a small region due to fibrosis or ischemia, with an electrical mass too small to be visibly detected in the global electrocardiogram signal.

Microvolt TWA is common in patients with cardiac diseases and its efficacy for risk stratification of arrhythmias and sudden death has been widely investigated.[13,29] Clinically, microvolt TWA testing has a higher negative predictive value than positive predictive value; that is, a negative test indicates a low probability of an event, whereas a positive test is less informative.[29]

T-wave lability

Although not as common as TWA, patients with heart disease can also exhibit T-wave lability, in which T-wave features vary irregularly from beat to beat (Figure 8H).[171] This appearance is consistent with the regional chaos synchronization mechanisms that come into play when dynamical chaos is present (Figure 6D).[44,47] For prolonged repolarization-induced arrhythmias, this occurs when the heart rate encounters the steep discontinuous region in the APDR curve at which EADs behave chaotically as illustrated in Figure 2B, causing regions with EADs to appear whose location in the tissue shifts irregularly from beat to beat (Figure 6D) such that the spatial repolarization sequence defining the features of each T-wave are different. The resulting dispersion of repolarization makes the tissue highly susceptible to initiation of reentry by both R-from-T and R-to-T mechanisms,[44,47] supporting the clinical observations of a high association between T-wave lability and Torsade de pointes episodes.[171–173]

A similar situation may occur with early repolarization-mediated arrhythmias, due to regional chaos

synchronization when the heart rate transitions from alternans into one of the nearby chaotic windows (Figure 2C). On the electrocardiogram, this would also manifest itself as T-wave lability reflecting marked underlying dispersion of repolarization from beat to beat, creating a vulnerable substrate with increased susceptibility to phase-2 reentry initiated by the R-from-T mechanism.

In CPVT, as well as normal and failing hearts, Ca-driven alternans or steep APDR slope-induced alternans can induce chaotic APD behavior when loss of 1:1 conduction occurs during sinus rhythm or non-reentrant VT, resulting in complex repolarization patterns and T-wave dynamics that facilitate initiation of reentry.

In summary, although T-wave lability is not as prevalent as TWA, when it occurs, it is even more arrhythmogenic due to the chaotic repolarization dynamics.

P-wave alternans

P-wave alternans, possibly the atrial equivalent of QRSA, has been observed only rarely in humans, and not clearly associated with atrial flutter or AF.[174] Atrial repolarization is not visible on a standard electrocardiogram, but atrial repolarization alternans has been detected during sinus rhythm or rapid pacing prior to AF initiation using intracardiac catheters in both humans[38,140,141] and animal experiments.[142–145]

Therapeutic Implications

With cardiac alternans serving both as an indicator of cardiac dynamical instability underlying high arrhythmia risk, as well as a direct causal mechanism that can initiate potentially lethal ventricular arrhythmias, targeting suppression of cardiac alternans pharmacologically or by other means is a promising antiarrhythmic strategy. However, with 3 categories of life-threatening arrhythmias to contend with, 5 underlying voltage- and Ca-driven mechanisms of alternans, and disease conditions that often involve multiple dynamic arrhythmia categories as well as multiple alternans mechanisms, the task of developing an effective strategy is not straightforward. In addition, lethal cardiac arrhythmias are also precipitated by other factors besides alternans, and interventions designed to suppress cardiac alternans must not exacerbate those other mechanisms of arrhythmogenesis. That said, the effects of some common antiarrhythmic drugs on cardiac alternans are summarized below.

Beta adrenergic blockers

For arrhythmias potentiated by adrenergic stimulation, such as CPVT, acute and chronic ischemia, some LQTS subtypes, beta blockers have multiple antiarrhythmic effects. These include: (1) slowing heart rate to avoid very short DIs that promote steep APDR slope-induced alternans, Ca-induced alternans and CVR-mediated SDA; (2) blunting adrenergic stimulation of LCCs that

promotes EADs, EAD-mediated alternans and chaotic APD dispersion promoting reentry initiation; (3) blunting adrenergic stimulation of SERCA pumps that increases SR Ca loading into the steep region of the fractional SR Ca release curve that promotes CaT alternans; (4) blunting adrenergic enhancement of RyR excitability and leakiness that promote Ca waves and DAD-mediated triggered activity; (5) reducing cardiac workload to attenuate the severity of acute myocardial ischemic episodes that can lead to early repolarization-induced alternans and phase-2 reentry. Generally, these effects make beta blockers safe as first-line antiarrhythmic therapy.

Na channel blockers

Na channel blockers decrease the amplitude and slow the recovery of the Na current,[175] altering both APDR and CVR such that alternans and SDA occur at slower heart rates,[176] particularly in the setting of acute and chronic ischemic heart disease in which the Na channel properties are already similarly altered by electrical remodeling.[177] This may have been an important factor contributing to the increased mortality in patients with ischemic heart disease treated with Na channel blockers in the Cardiac Arrhythmia Suppression Trial (CAST).[178] Blocking Na channels can promote early repolarization-induced alternans, which may contribute to inducing TWA in Brugada syndrome.[135,179–181] A more promising class of Na channel blockers, however, may be selective late Na channel blockers that shorten the QT interval, abolish TWA, and suppress arrhythmias in patients with LQTS.[21,182]

Ca channel blockers

High doses of Ca channel blockers shorten APD and flatten APDR slope, and thus can suppress steep APDR slope-induced alternans. Ca channel blockers also suppress EADs and EAD-induced alternans. However, the high dosages required often suppress contractility too severely to be useful clinically. Similar to Na channel blockers, Ca channel blockers can promote early repolarization-induced alternans and phase-2 reentry in Brugada syndrome. Blocking Ca channels can either promote or suppress Ca-driven alternans depending on the setting,[63,80,92] as has been observed with verapamil.[141,183–185] Drugs that block the Ca window current selectively without reducing its peak amplitude, although not yet clinically available, have been shown to suppress EADs and prolonged repolarization-induced alternans without unduly suppressing the CaT and contractility.[43,48,125,186] They may also be effective at suppressing early repolarization-induced alternans and the early repolarization-induced instability.[187]

K channel blockers and openers

K channel blockers lengthen APD and steepen APDR slope, promoting steep APDR slope-induced alternans.

K channel blockers also promote EADs and EAD-induced alternans, which may have contributed to the increased mortality in patients with ischemic heart disease treated with d-sotalol in the Survival With ORal D-sotalol (SWORD) trial.[188] For early repolarization-induced alternans, blocking K currents, particularly I_{to} (eg, with low dose quinidine), suppresses alternans. The effects of K channel blockers on Ca-driven alternans are still unclear. K channel openers have been shown to suppress voltage-driven alternans by flattening APDR slope[189] and suppressing EADs in the setting of LQTS.[190,191]

SERCA overexpression

It has been shown that overexpressing SERCA suppresses both mechanisms of Ca-driven alternans.[81,96] However, increasing SERCA activity can overload the SR, which increases the susceptibility to Ca waves and thus DAD-induced triggered activity.

SUMMARY

We have reviewed how an astute clinical observation was the starting point for a 150 year bedside-to-bench-and-back-again journey involving exemplary collaborative science by multiple generations clinicians, experimental and theoretical biologists. Unraveling cardiac alternans has been a vital step leading to deeper understanding of the dynamics of cardiac arrhythmias that can end the lives of patients across a wide spectrum inherited and acquired human cardiovascular diseases. It is complicated, with 3 voltage-driven and 2 Ca-driven mechanisms that serve as warning signs that the heart is nearing the threshold for more complex instabilities that can degenerate into serious ventricular and atrial arrhythmias. As such, alternans is a common precursor to all 3 of the major categories of cardiac arrhythmias, including disorders of Ca cycling, prolonged repolarization, and early repolarization, spanning inherited diseases such as CPVT, LQTS, short QT syndromes, and Brugada syndrome to common diseases such as acute and chronic myocardial ischemia, heart failure, and drug toxicity. Not only is cardiac alternans an early warning sign of more life-threatening cardiac instabilities to come, but also plays a direct causal role in initiating reentry, by creating a vulnerable substrate for reentry initiation by exogenous PVCs arising via the R-to-T mechanism or by PVCs self-generated by the repolarization gradients via the R-from-T mechanism. The multifactorial nature of cardiac alternans and its involvement in multiple arrhythmia mechanisms make it a daunting antiarrhythmic target, but a highly worthwhile goal for the upcoming generation of scientists and clinicians to pursue in the same collaborative spirit.

REFERENCES

1. Traube L. Ein Fall von Pulsus bigeminus nebst Bemerkungen uber die Leberschwellungen bei Klappenfehlern und acute Leberatrophie. *Ber. Klin. Wschr.* 1872;9:185.
2. Hering HE. Experimentelle Studien an Saugentieren uber das Electrocardiogram. *Z Exp Med.* 1909;7:363–378.
3. Lewis T. Notes upon alternation of the heart. *Quart. J. Med* 1910;4:141–144.
4. Cohn KE, Sandler H, Hancock EW. Mechanisms of pulsus alternans. *Circulation* 1967;36:372–380. doi: 10.1161/01.cir.36.3.372
5. Surawicz B, Fisch C. Cardiac alternans: diverse mechanisms and clinical manifestations. *J Am Coll Cardiol.* 1992;20:483–499. doi: 10.1016/0735-1097(92)90122-4
6. Rosenbaum DS, Albrecht P, Cohen RJ. Predicting sudden cardiac death from T wave alternans of the surface electrocardiogram: promise and pitfalls. *J Cardiovasc Electrophysiol.* 1996;7:1095–1111. doi: 10.1111/j.1540-8167.1996.tb00487.x
7. Euler DE. Cardiac alternans: mechanisms and pathophysiological significance. *Cardiovasc Res.* 1999;42:583–590. doi: 10.1016/s0008-6363(99)00011-5
8. Rosenbaum DS. T wave alternans: a mechanism of arrhythmogenesis comes of age after 100 years. *J Cardiovasc Electrophysiol.* 2001;12:207–209. doi: 10.1046/j.1540-8167.2001.00207.x
9. Walker ML, Rosenbaum DS. Repolarization alternans: implications for the mechanism and prevention of sudden cardiac death. *Cardiovasc Res.* 2003;57:599–614. doi: 10.1016/s0008-6363(02)00737-x
10. Weiss JN, Karma A, Shiferaw Y, Chen PS, Garfinkel A, Qu Z. From pulsus to pulseless: the saga of cardiac alternans. *Circ Res.* 2006;98:1244–1253. doi: 10.1161/01.RES.0000224540.97431.f0
11. Narayan SM. T-wave alternans and the susceptibility to ventricular arrhythmias. *J Am Coll Cardiol.* 2006;47:269–281. doi: 10.1016/j.jacc.2005.08.066
12. Qu Z, Xie Y, Garfinkel A, Weiss JN. T-wave alternans and arrhythmogenesis in cardiac diseases. *Front Physiol.* 2010;1:154. doi: 10.3389/fphys.2010.00154
13. Armoundas AA, Tomaselli GF, Esperer HD. Pathophysiological basis and clinical application of T-wave alternans. *J Am Coll Cardiol.* 2002;40:207–217. doi: 10.1016/s0735-1097(02)01960-5
14. Rosenbaum DS. T-wave alternans in the sudden cardiac death in heart failure trial population: signal or noise? *Circulation* 2008;118:2015–2018. doi: 10.1161/CIRCULATIONAHA.108.818286
15. Rosenbaum DS, Jackson LE, Smith JM, Garan H, Ruskin JN, Cohen RJ. Electrical alternans and vulnerability to ventricular arrhythmias. *N Engl J Med.* 1994;330:235–241. doi: 10.1056/NEJM199401273300402
16. Gehi AK, Stein RH, Metz LD, Gomes JA. Microvolt T-wave alternans for the risk stratification of ventricular tachyarrhythmic events: a meta-analysis. *J Am Coll Cardiol.* 2005;46:75–82. doi: 10.1016/j.jacc.2005.03.059
17. Zareba W, Moss AJ, le Cessie S, Hall WJ. T wave alternans in idiopathic long QT syndrome. *J Am Coll Cardiol.* 1994;23:1541–1546. doi: 10.1016/0735-1097(94)90653-x
18. Armoundas AA, Nanke T, Cohen RJ. Images in cardiovascular medicine. T-wave alternans preceding torsade de pointes ventricular tachycardia. *Circulation* 2000;101:2550. doi: 10.1161/01.cir.101.21.2550
19. Crotti L, Celano G, Dagradi F, Schwartz PJ. Congenital long QT syndrome. *Orphanet J Rare Dis.* 2008;3:18. doi: 10.1186/1750-1172-3-18

20. Liu T, Patel C, Guo D, Ju R, Kowey P, Yan G-X. Early afterdepolarization alternans manifests T wave alternans in left ventricular hypertrophy. *Circulation* 2013;128:A10368.

21. Badri M, Patel A, Patel C, Liu G, Goldstein M, Robinson VM, Xue X, Yang L, Kowey PR, Yan G-X. Mexiletine prevents recurrent torsades de pointes in acquired long QT syndrome refractory to conventional measures. *JACC Clin Electrophysiol* 2015;1:315–322. doi: 10.1016/j.jacep.2015.05.008

22. Soma D, Johnson B, Rosenblum A. Macrovolt T-wave alternans: A foreboding sign for ventricular arrhythmia in severe systemic illness. *J Am Coll Cardiol*. 2020;75:2693–2693. doi: 10.1016/s0735-1097(20)33320-9

23. Omondi A, Sirinvaravong N, Spears J, Sauerwein S, Taoutel R, Liskov S, Gao C, Liu T, Kowey PR, Yan G-X. Marked QTc reduction immediately following direct current cardioversion of atrial fibrillation: Clinical implications and mechanisms [published online August 13, 2022]. *JACC Clin Electrophysiol*. doi: 10.2139/ssrn.4189335. https://ssrn.com/abstract=4189335

24. Wegener FT, Ehrlich JR, Hohnloser SH. Amiodarone-associated macroscopic T-wave alternans and torsade de pointes unmasking the inherited long QT syndrome. *Europace* 2008;10:112–113. doi: 10.1093/europace/eum252

25. Drew BJ, Ackerman MJ, Funk M, Gibler WB, Kligfield P, Menon V, Philippides GJ, Roden DM, Zareba W; American Heart Association Acute Cardiac Care Committee of the Council on Clinical Cardiology, the Council on Cardiovascular Nursing, and the American College of Cardiology Foundation. Prevention of torsade de pointes in hospital settings: a scientific statement from the American Heart Association and the American College of Cardiology Foundation. *Circulation* 2010;121:1047–1060. doi: 10.1161/CIRCULATIONAHA.109.192704

26. Holley CL, Cooper JA. Macrovolt T-wave alternans and polymorphic ventricular tachycardia. *Circulation* 2009;120:445–446. doi: 10.1161/CIRCULATIONAHA.109.861633

27. Schwartz PJ, Crotti L. QTc behavior during exercise and genetic testing for the long-QT syndrome. *Circulation* 2011;124:2181–2184. doi: 10.1161/CIRCULATIONAHA.111.062182

28. Fishman GI, Chugh SS, Dimarco JP, Albert CM, Anderson ME, Bonow RO, Buxton AE, Chen PS, Estes M, Jouven X, et al. Sudden cardiac death prediction and prevention: report from a national heart, lung, and blood institute and heart rhythm society workshop. *Circulation* 2010;122:2335–2348. doi: 10.1161/CIRCULATIONAHA.110.976092

29. Verrier RL, Klingenheben T, Malik M, El-Sherif N, Exner DV, Hohnloser SH, Ikeda T, Martinez JP, Narayan SM, Nieminen T, et al. Microvolt T-wave alternans physiological basis, methods of measurement, and clinical utility—consensus guideline by International Society for Holter and Noninvasive Electrocardiology. *J Am Coll Cardiol*. 2011;58:1309–1324. doi: 10.1016/j.jacc.2011.06.029

30. Weiss JN, Garfinkel A, Karagueuzian HS, Nguyen TP, Olcese R, Chen PS, Qu Z. Perspective: a dynamics-based classification of ventricular arrhythmias. *J Mol Cell Cardiol*. 2015;82:136–152.

31. Nolasco JB, Dahlen RW. A graphic method for the study of alternation in cardiac action potentials. *J Appl Physiol*. 1968;25:191–196. doi: 10.1152/jappl.1968.25.2.191

32. Huang C, Song Z, Landaw J, Qu Z. Spatially discordant repolarization alternans in the absence of conduction velocity restitution. *Biophys J*. 2020;118:2574–2587. doi: 10.1016/j.bpj.2020.02.008

33. Qu Z, Xie F, Garfinkel A, Weiss JN. Origins of spiral wave meander and breakup in a two-dimensional cardiac tissue model. *Ann Biomed Eng*. 2000;28:755–771. doi: 10.1114/1.1289474

34. Franz MR, Schaefer J, Schottler M, Seed WA, Noble MIM. Electrical and mechanical restitution of the human heart at different rates of stimulation. *Circ Res*. 1983;53:815–822. doi: 10.1161/01.res.53.6.815

35. Morad M, Goldman Y. Excitation-contraction coupling in heart muscle: membrane control of development of tension. *Prog Biophys Mol Biol*. 1973;27:257–313. doi: 10.1016/0079-6107(73)90008-4

36. Pruvot EJ, Katra RP, Rosenbaum DS, Laurita KR. Role of calcium cycling versus restitution in the mechanism of repolarization alternans. *Circ Res*. 2004;94:1083–1090. doi: 10.1161/01.RES.0000125629.72053.95

37. Goldhaber JI, Xie LH, Duong T, Motter C, Khuu K, Weiss JN. Action potential duration restitution and alternans in rabbit ventricular myocytes: the key role of intracellular calcium cycling. *Circ Res*. 2005;96:459–466. doi: 10.1161/01.RES.0000156891.66893.83

38. Narayan SM, Franz MR, Clopton P, Pruvot EJ, Krummen DE. Repolarization alternans reveals vulnerability to human atrial fibrillation. *Circulation* 2011;123:2922–2930. doi: 10.1161/CIRCULATIONAHA.110.977827

39. Zhou X, Bueno-Orovio A, Orini M, Hanson B, Hayward M, Taggart P, Lambiase PD, Burrage K, Rodriguez B. In vivo and in silico investigation into mechanisms of frequency dependence of repolarization alternans in human ventricular cardiomyocytes. *Circ Res*. 2016;118:266–278. doi: 10.1161/CIRCRESAHA.115.307836

40. Elharrar V, Surawicz B. Cycle length effect on restitution of action potential duration in dog cardiac fibers. *Am J Physiol*. 1983;244:H782–H792. doi: 10.1152/ajpheart.1983.244.6.H782

41. Fox JJ, Bodenschatz E, Gilmour RF. Period-doubling instability and memory in cardiac tissue. *Phys Rev Lett*. 2002;89:138101. doi: 10.1103/PhysRevLett.89.138101

42. Roden DM. Taking the "Idio" out of "Idiosyncratic": predicting torsades de pointes. *Pacing Clin Electrophysiol*. 1998;21:1029–1034. doi: 10.1111/j.1540-8159.1998.tb00148.x

43. Qu Z, Xie L-H, Olcese R, Karagueuzian HS, Chen P-S, Garfinkel A, Weiss JN. Early afterdepolarizations in cardiac myocytes: beyond reduced repolarization reserve. *Cardiovasc Res*. 2013;99:6–15. doi: 10.1093/cvr/cvt104

44. Sato D, Xie LH, Sovari AA, Tran DX, Morita N, Xie F, Karagueuzian H, Garfinkel A, Weiss JN, Qu Z. Synchronization of chaotic early afterdepolarizations in the genesis of cardiac arrhythmias. *Proc Natl Acad Sci USA*. 2009;106:2983–2988. doi: 10.1073/pnas.0809148106

45. Sato D, Xie LH, Nguyen TP, Weiss JN, Qu Z. Irregularly appearing early afterdepolarizations in cardiac myocytes: random fluctuations or dynamical chaos? *Biophys J*. 2010;99:765–773. doi: 10.1016/j.bpj.2010.05.019

46. Landaw J, Qu Z. Memory-induced nonlinear dynamics of excitation in cardiac diseases. *Phys Rev E* 2018;97:042414. doi: 10.1103/PhysRevE.97.042414

47. Liu W, Kim TY, Huang X, Liu MB, Koren G, Choi BR, Qu Z. Mechanisms linking T-wave alternans to spontaneous initiation of ventricular arrhythmias in rabbit models of long QT syndrome. *J Physiol*. 2018;596:1341–1355. doi: 10.1113/JP275492

48. Qu Z, Chung D. Mechanisms and determinants of ultralong action potential duration and slow rate-dependence in cardiac myocytes. *PLoS One*. 2012;7:e43587. doi: 10.1371/journal.pone.0043587

49. Lukas A, Antzelevitch C. Differences in the electrophysiological response of canine ventricular epicardium and endocardium to ischemia. Role of the transient outward current. *Circulation* 1993;88:2903–2915. doi: 10.1161/01.cir.88.6.2903

50. Morita H, Zipes DP, Lopshire J, Morita ST, Wu J. T wave alternans in an in vitro canine tissue model of Brugada syndrome. *Am J Physiol Heart Circ Physiol*. 2006;291:H421–H428. doi: 10.1152/ajpheart.01259.2005

51. Fish JM, Antzelevitch C. Cellular mechanism and arrhythmogenic potential of T-wave alternans in the Brugada syndrome. *J Cardiovasc Electrophysiol*. 2008;19:301–308. doi: 10.1111/j.1540-8167.2007.01025.x

52. Hopenfeld B. Mechanism for action potential alternans: the interplay between L-type calcium current and transient outward current. *Heart Rhythm* 2006;3:345–352. doi: 10.1016/j.hrthm.2005.11.016

53. Clancy CE, Rudy Y. Na(+) channel mutation that causes both Brugada and long-QT syndrome phenotypes: a simulation study of mechanism. *Circulation* 2002;105:1208–1213. doi: 10.1161/hc1002.105183

54. Guevara MR, Ward G, Shrier A, Glass L. Electrical alternans and period doubling bifurcations. *IEEE Comp. Cardiol*. 1984;562:167–170.

55. Chialvo DR, Gilmour RF, Jalife J. Low dimensional chaos in cardiac tissue. *Nature* 1990;343:653–657. doi: 10.1038/343653a0

56. Qu Z, Shiferaw Y, Weiss JN. Nonlinear dynamics of cardiac excitation-contraction coupling: an iterated map study. *Phys Rev E* 2007;75:011927.

57. Qu Z, Hu G, Garfinkel A, Weiss JN. Nonlinear and stochastic dynamics in the heart. *Phys Rep*. 2014;543:61–162. doi: 10.1016/j.physrep.2014.05.002

58. Chudin E, Goldhaber J, Garfinkel A, Weiss J, Kogan B. Intracellular Ca2+ dynamics and the stability of ventricular tachycardia. *Biophys J*. 1999;77:2930–2941. doi: 10.1016/S0006-3495(99)77126-2

59. Diaz ME, Eisner DA, O'Neill SC. Depressed ryanodine receptor activity increases variability and duration of the systolic Ca2+ transient in rat ventricular myocytes. *Circ Res*. 2002;91:585–593. doi: 10.1161/01.res.0000035527.53514.c2

60. Diaz ME, O'Neill SC, Eisner DA. Sarcoplasmic reticulum calcium content fluctuation is the key to cardiac alternans. *Circ Res*. 2004;94:650–656. doi: 10.1161/01.RES.0000119923.64774.72

61. Kanaporis G, Blatter LA. The mechanisms of calcium cycling and action potential dynamics in cardiac alternans. *Circ Res*. 2015;116:846–856. doi: 10.1161/CIRCRESAHA.116.305404

62. Baddeley D, Jayasinghe ID, Lam L, Rossberger S, Cannell MB, Soeller C. Optical single-channel resolution imaging of the ryanodine receptor distribution in rat cardiac myocytes. *Proc Natl Acad Sci USA*. 2009;106:22275–22280. doi: 10.1073/pnas.0908971106

REVIEW

63. Rovetti R, Cui X, Garfinkel A, Weiss JN, Qu Z. Spark-induced sparks as a mechanism of intracellular calcium alternans in cardiac myocytes. *Circ Res.* 2010;106:1582–1591. doi: 10.1161/CIRCRESAHA.109.213975

64. Cheng H, Lederer MR, Lederer WJ, Cannell MB. Calcium sparks and [Ca2+]i waves in cardiac myocytes. *Am J Physiol.* 1996;270:C148–C159. doi: 10.1152/ajpcell.1996.270.1.C148

65. Wier WG, ter Keurs HE, Marban E, Gao WD, Balke CW. Ca2+ "sparks" and waves in intact ventricular muscle resolved by confocal imaging. *Circ Res.* 1997;81:462–469. doi: 10.1161/01.res.81.4.462

66. Nivala M, de Lange E, Rovetti R, Qu Z. Computational modeling and numerical methods for spatiotemporal calcium cycling in ventricular myocytes. *Front Physiol.* 2012;3:114. doi: 10.3389/fphys.2012.00114

67. Weiss JN, Nivala M, Garfinkel A, Qu Z. Alternans and arrhythmias: from cell to heart. *Circ Res.* 2011;108:98–112. doi: 10.1161/circresaha.110.223586

68. Qu Z, Liu MB, Nivala M. A unified theory of calcium alternans in ventricular myocytes. *Sci Rep.* 2016;6:35625. doi: 10.1038/srep35625

69. Shannon TR, Ginsburg KS, Bers DM. Potentiation of fractional sarcoplasmic reticulum calcium release by total and free intra-sarcoplasmic reticulum calcium concentration. *Biophys J.* 2000;78:334–343. doi: 10.1016/S0006-3495(00)76596-9

70. Brochet DX, Yang D, Di Maio A, Lederer WJ, Franzini-Armstrong C, Cheng H. Ca2+ blinks: rapid nanoscopic store calcium signaling. *Proc Natl Acad Sci USA.* 2005;102:3099–3104. doi: 10.1073/pnas.0500059102

71. Ramay HR, Liu OZ, Sobie EA. Recovery of cardiac calcium release is controlled by sarcoplasmic reticulum refilling and ryanodine receptor sensitivity. *Cardiovasc Res.* 2011;91:598–605. doi: 10.1093/cvr/cvr143

72. Cely-Ortiz A, Felice JI, Díaz-Zegarra LA, Valverde CA, Federico M, Palomeque J, Wehrens XHT, Kranias EG, Aiello EA, Lascano EC, et al. Determinants of Ca2+ release restitution: Insights from genetically altered animals and mathematical modeling. *J Gen Physiol.* 2020;152:e201912512. doi: 10.1085/jgp.201912512

73. Zima AV, Picht E, Bers DM, Blatter LA. Termination of cardiac Ca2+ sparks: role of intra-SR [Ca2+], release flux, and intra-SR Ca2+ diffusion. *Circ Res.* 2008;103:e105–e115. doi: 10.1161/CIRCRESAHA.107.183236

74. Chen W, Wang R, Chen B, Zhong X, Kong H, Bai Y, Zhou Q, Xie C, Zhang J, Guo A, et al. The ryanodine receptor store-sensing gate controls Ca2+ waves and Ca2+-triggered arrhythmias. *Nat Med.* 2014;20:184–192. doi: 10.1038/nm.3440

75. Gyorke I, Hester N, Jones LR, Gyorke S. The role of calsequestrin, triadin, and junctin in conferring cardiac ryanodine receptor responsiveness to luminal calcium. *Biophys J.* 2004;86:2121–2128. doi: 10.1016/S0006-3495(04)74271-X

76. Eisner DA, Choi HS, Diaz ME, O'Neill SC, Trafford AW. Integrative analysis of calcium cycling in cardiac muscle. *Circ Res.* 2000;87:1087–1094. doi: 10.1161/01.res.87.12.1087

77. Shiferaw Y, Watanabe MA, Garfinkel A, Weiss JN, Karma A. Model of intracellular calcium cycling in ventricular myocytes. *Biophys J.* 2003; 85:3666–3686. doi: 10.1016/S0006-3495(03)74784-5

78. Restrepo JG, Weiss JN, Karma A. Calsequestrin-mediated mechanism for cellular calcium transient alternans. *Biophys J.* 2008;95:3767–3789. doi: 10.1529/biophysj.108.130419

79. Nivala M, Qu Z. Calcium alternans in a couplon network model of ventricular myocytes: Role of sarcoplasmic reticulum load. *Am J Physiol Heart Circ Physiol.* 2012;303:H341–H352. doi: 10.1152/ajpheart.00302.2012

80. Li Y, Diaz ME, Eisner DA, O'Neill S. The effects of membrane potential, SR Ca2+ content and RyR responsiveness on systolic Ca2+ alternans in rat ventricular myocytes. *J Physiol.* 2009;587:1283–1292. doi: 10.1113/jphysiol.2008.164368

81. Xie LH, Sato D, Garfinkel A, Qu Z, Weiss JN. Intracellular Ca alternans: coordinated regulation by sarcoplasmic reticulum release, uptake, and leak. *Biophys J.* 2008;95:3100–3110. doi: 10.1529/biophysj.108.130955

82. Nivala M, Song Z, Weiss JN, Qu Z. T-tubule disruption promotes calcium alternans in failing ventricular myocytes: Mechanistic insights from computational modeling. *J Mol Cell Cardiol.* 2015;79:32–41. doi: 10.1016/j.yjmcc.2014.10.018

83. Huser J, Wang YG, Sheehan KA, Cifuentes F, Lipsius SL, Blatter LA. Functional coupling between glycolysis and excitation-contraction coupling underlies alternans in cat heart cells. *J Physiol.* 2000;524:795–806. doi: 10.1111/j.1469-7793.2000.00795.x

84. Picht E, DeSantiago J, Blatter LA, Bers DM. Cardiac alternans do not rely on diastolic sarcoplasmic reticulum calcium content fluctuations. *Circ Res.* 2006;99:740–748. doi: 10.1161/01.RES.0000244002.88813.91

85. Shkryl VM, Maxwell JT, Domeier TL, Blatter LA. Refractoriness of sarcoplasmic reticulum Ca release determines Ca alternans in atrial myocytes. *Am J Physiol Heart Circ Physiol.* 2012;302:H2310–H2320. doi: 10.1152/ajpheart.00079.2012

86. Wang L, Myles RC, Jesus NMD, Ohlendorf AKP, Bers DM, Ripplinger CM. Optical Mapping of Sarcoplasmic Reticulum Ca2+ in the Intact Heart. *Circ Res.* 2014;114:1410–1421.

87. Zhong X, Sun B, Vallmitjana A, Mi T, Guo W, Ni M, Wang R, Guo A, Duff HJ, Gillis AM, et al. Suppression of ryanodine receptor function prolongs Ca2+ release refractoriness and promotes cardiac alternans in intact hearts. *Biochem J.* 2016;473:3951–3964.

88. Wei J, Yao J, Belke D, Guo W, Zhong X, Sun B, Wang R, Estillore JP, Vallmitjana A, Benitez R, et al. Ca2+-CaM Dependent Inactivation of RyR2 Underlies Ca2+ Alternans in Intact Heart. *Circ Res.* 2021;128:e63–e83.

89. Liu T, Xiong F, Qi X-Y, Xiao J, Villeneuve L, Abu-Taha I, Dobrev D, Huang C, Nattel S. Altered calcium handling produces reentry-promoting action potential alternans in atrial fibrillation–remodeled hearts. *JCI Insight* 2020;5:e133754. doi: 10.1172/jci.insight.133754

90. Tian Q, Kaestner L, Lipp P. Noise-free visualization of microscopic calcium signaling by pixel-wise fitting. *Circ Res.* 2012;111:17–27. doi: 10.1161/CIRCRESAHA.112.266403

91. Belevych AE, Terentyev D, Viatchenko-Karpinski S, Terentyeva R, Sridhar A, Nishijima Y, Wilson LD, Cardounel AJ, Laurita KR, Carnes CA, et al. Redox modification of ryanodine receptors underlies calcium alternans in a canine model of sudden cardiac death. *Cardiovasc Res.* 2009; 84:387–395. doi: 10.1093/cvr/cvp246

92. Song Z, Liu MB, Qu Z. Transverse tubular network structures in the genesis of intracellular calcium alternans and triggered activity in cardiac cells. *J Mol Cell Cardiol.* 2018;114:288–299. doi: 10.1016/j.yjmcc.2017.12.003

93. Tao T, O'Neill SC, Diaz ME, Li YT, Eisner DA, Zhang H. Alternans of cardiac calcium cycling in a cluster of ryanodine receptors: a simulation study. *Am J Physiol Heart Circ Physiol.* 2008;295:H598–H609. doi: 10.1152/ajpheart.01086.2007

94. Wan X, Laurita KR, Pruvot EJ, Rosenbaum DS. Molecular correlates of repolarization alternans in cardiac myocytes. *J Mol Cell Cardiol.* 2005;39:419–428. doi: 10.1016/j.yjmcc.2005.06.004

95. Wilson LD, Jeyaraj D, Wan X, Hoeker GS, Said TH, Gittinger M, Laurita KR, Rosenbaum DS. Heart failure enhances susceptibility to arrhythmogenic cardiac alternans. *Heart Rhythm* 2009;6:251–259. doi: 10.1016/j.hrthm.2008.11.008

96. Cutler MJ, Wan X, Laurita KR, Hajjar RJ, Rosenbaum DS. Targeted SERCA2a Gene Expression Identifies Molecular Mechanism and Therapeutic Target for Arrhythmogenic Cardiac Alternans. *Circ Arrhythm Electrophysiol* 2009;2:686–694. doi: 10.1161/CIRCEP.109.863118

97. Song LS, Sobie EA, McCulle S, Lederer WJ, Balke CW, Cheng H. Orphaned ryanodine receptors in the failing heart. *Proc Natl Acad Sci USA.* 2006;103:4305–4310. doi: 10.1073/pnas.0509324103

98. Wei S, Guo A, Chen B, Kutschke W, Xie YP, Zimmerman K, Weiss RM, Anderson ME, Cheng H, Song LS. T-tubule remodeling during transition from hypertrophy to heart failure. *Circ Res.* 2010;107:520–531. doi: 10.1161/CIRCRESAHA.109.212324

99. Sachse FB, Torres NS, Savio-Galimberti E, Aiba T, Kass DA, Tomaselli GF, Bridge JH. Subcellular structures and function of myocytes impaired during heart failure are restored by cardiac resynchronization therapy. *Circ Res.* 2012;110:588–597. doi: 10.1161/CIRCRESAHA.111.257428

100. Chen-Izu Y, Ward CW, Stark W Jr, Banyasz T, Sumandea MP, Balke CW, Izu LT, Wehrens XH. Phosphorylation of RyR2 and shortening of RyR2 cluster spacing in spontaneously hypertensive rat with heart failure. *Am J Physiol Heart Circ Physiol.* 2007;293:H2409–H2417. doi: 10.1152/ajpheart.00562.2007

101. Kockskamper J, Blatter LA. Subcellular Ca2+ alternans represents a novel mechanism for the generation of arrhythmogenic Ca2+ waves in cat atrial myocytes. *J Physiol.* 2002;545:65–79. doi: 10.1113/jphysiol.2002.025502

102. Gaeta SA, Bub G, Abbott GW, Christini DJ. Dynamical mechanism for subcellular alternans in cardiac myocytes. *Circ Res.* 2009; 105:335–342. doi: 10.1161/CIRCRESAHA.109.197590

103. Aistrup GL, Shiferaw Y, Kapur S, Kadish AH, Wasserstrom JA. Mechanisms underlying the formation and dynamics of subcellular calcium alternans in the intact rat heart. *Circ Res.* 2009;104:639–649. doi: 10.1161/CIRCRESAHA.108.181909

104. Xie LH, Weiss JN. Arrhythmogenic consequences of intracellular calcium waves. *Am J Physiol Heart Circ Physiol.* 2009;297:H997–H1002. doi: 10.1152/ajpheart.00390.2009

105. Shiferaw Y, Karma A. Turing instability mediated by voltage and calcium diffusion in paced cardiac cells. *Proc Natl Acad Sci USA.* 2006;103:5670–5675. doi: 10.1073/pnas.0511061103

REVIEW

106. Song Z, Qu Z. Delayed global feedback in the genesis and stability of spatiotemporal excitation patterns in paced biological excitable media. *PLoS Comput Biol.* 2020;16:e1007931. doi: 10.1371/journal.pcbi.1007931

107. Chua SK, Chang PC, Maruyama M, Turker I, Shinohara T, Shen MJ, Chen Z, Shen C, Rubart-von der Lohe M, Lopshire JC, et al. Small-conductance calcium-activated potassium channel and recurrent ventricular fibrillation in failing rabbit ventricles. *Circ Res.* 2011;108:971–979. doi: 10.1161/CIRCRESAHA.110.238386

108. Zhang X-D, Lieu DK, Chiamvimonvat N. Small-conductance Ca2+-activated K+ channels and cardiac arrhythmias. *Heart Rhythm* 2015;12:1845–1851. doi: 10.1016/j.hrthm.2015.04.046

109. Wan X, Cutler M, Song Z, Karma A, Matsuda T, Baba A, Rosenbaum DS. New experimental evidence for mechanism of arrhythmogenic membrane potential alternans based on balance of electrogenic INCX/ICa currents. *Heart Rhythm* 2012;9:1698–1705. doi: 10.1016/j.hrthm.2012.06.031

110. Shiferaw Y, Sato D, Karma A. Coupled dynamics of voltage and calcium in paced cardiac cells. *Phys Rev E* 2005;71:021903.

111. Wisialowski T, Crimin K, Engtrakul J, O'Donnell J, Fermini B, Fossa AA. Differentiation of arrhythmia risk of the antibacterials moxifloxacin, erythromycin, and telithromycin based on analysis of monophasic action potential duration alternans and cardiac instability. *J Pharmacol Exp Ther.* 2006;318:352–359. doi: 10.1124/jpet.106.101881

112. Cao JM, Qu Z, Kim YH, Wu TJ, Garfinkel A, Weiss JN, Karagueuzian HS, Chen PS. Spatiotemporal heterogeneity in the induction of ventricular fibrillation by rapid pacing: importance of cardiac restitution properties. *Circ Res.* 1999;84:1318–1331. doi: 10.1161/01.res.84.11.1318

113. Pastore JM, Girouard SD, Laurita KR, Akar FG, Rosenbaum DS. Mechanism linking T-wave alternans to the genesis of cardiac fibrillation. *Circulation* 1999;99:1385–1394. doi: 10.1161/01.cir.99.10.1385

114. Qu Z, Garfinkel A, Chen PS, Weiss JN. Mechanisms of discordant alternans and induction of reentry in simulated cardiac tissue. *Circulation* 2000;102:1664–1670. doi: 10.1161/01.cir.102.14.1664

115. Watanabe MA, Fenton FH, Evans SJ, Hastings HM, Karma A. Mechanisms for discordant alternans. *J Cardiovasc Electrophysiol.* 2001;12:196–206. doi: 10.1046/j.1540-8167.2001.00196.x

116. Hayashi H, Shiferaw Y, Sato D, Nihei M, Lin SF, Chen PS, Garfinkel A, Weiss JN, Qu Z. Dynamic origin of spatially discordant alternans in cardiac tissue. *Biophys J.* 2007;92:448–460. doi: 10.1529/biophysj.106.091009

117. de Diego C, Pai RK, Dave AS, Lynch A, Thu M, Chen F, Xie LH, Weiss JN, Valderrabano M. Spatially discordant alternans in cardiomyocyte monolayers. *Am J Physiol Heart Circ Physiol.* 2008;294:H1417–H1425. doi: 10.1152/ajpheart.01233.2007

118. Mironov S, Jalife J, Tolkacheva EG. Role of conduction velocity restitution and short-term memory in the development of action potential duration alternans in isolated rabbit hearts. *Circulation* 2008;118:17–25. doi: 10.1161/CIRCULATIONAHA.107.737254

119. Banville I, Gray RA. Effect of action potential duration and conduction velocity restitution and their spatial dispersion on alternans and the stability of arrhythmias. *J Cardiovasc Electrophysiol.* 2002;13:1141–1149. doi: 10.1046/j.1540-8167.2002.01141.x

120. Gizzi A, Cherry EM, Gilmour RF Jr, Luther S, Filippi S, Fenton FH. Effects of pacing site and stimulation history on alternans dynamics and the development of complex spatiotemporal patterns in cardiac tissue. *Front Physiol.* 2013;4:71. doi: 10.3389/fphys.2013.00071

121. Ziv O, Morales E, Song YK, Peng X, Odening KE, Buxton AE, Karma A, Koren G, Choi BR. Origin of complex behaviour of spatially discordant alternans in a transgenic rabbit model of type 2 long QT syndrome. *J Physiol.* 2009;587:4661–4680. doi: 10.1113/jphysiol.2009.175018

122. Lau E, Kossidas K, Kim TY, Kunitomo Y, Ziv O, Song Z, Taylor C, Schofield L, Yammine J, Liu G, et al. Spatially discordant alternans and arrhythmias in tachypacing-induced cardiac myopathy in transgenic LQT1 rabbits: The importance of IKs and Ca2+ cycling. *PLoS One.* 2015;10:e01321 98e0122754. doi: 10.1371/journal.pone.0132198

123. Huang C, Song Z, Qu Z. Synchronization of spatially discordant voltage and calcium alternans in cardiac tissue. *Phys Rev E* 2022;106:024406. doi: 10.1103/PhysRevE.106.024406

124. Boyden PA, Dun W, Stuyvers BD. What is a Ca2+ wave? Is it like an Electrical Wave?. *Arrhythm Electrophysiol Rev* 2015;4:35–39. doi: 10.15420/aer.2015.4.1.35

125. Liu MB, Vandersickel N, Panfilov AV, Qu Z. R-from-T as a common mechanism of arrhythmia initiation in long QT syndromes. *Circ Arrhythm Electrophysiol* 2019;12:e007571. doi: 10.1161/CIRCEP.119.007571

126. Qu Z, Liu MB, Olcese R, Karagueuzian H, Garfinkel A, Chen P-S, Weiss JN. R-on-T and the initiation of reentry revisited: Integrating old and new concepts. *Heart Rhythm* 2022;19:1369–1383. doi: 10.1016/j.hrthm.2022.03.1224

127. Liu N, Priori SG. Disruption of calcium homeostasis and arrhythmogenesis induced by mutations in the cardiac ryanodine receptor and calsequestrin. *Cardiovasc Res.* 2008;77:293–301. doi: 10.1093/cvr/cvm004

128. Priori SG, Chen SRW. Inherited Dysfunction of Sarcoplasmic Reticulum Ca2+ Handling and Arrhythmogenesis. *Circ Res.* 2011;108:871–883. doi: 10.1161/CIRCRESAHA.110.226845

129. Walker ML, Wan X, Kirsch GE, Rosenbaum DS. Hysteresis effect implicates calcium cycling as a mechanism of repolarization alternans. *Circulation* 2003;108:2704–2709. doi: 10.1161/01.CIR.0000093276.10885.5B

130. Liu MB, de Lange E, Garfinkel A, Weiss JN, Qu Z. Delayed afterdepolarizations generate both triggers and a vulnerable substrate promoting reentry in cardiac tissue. *Heart Rhythm* 2015;12:2115–2124. doi: 10.1016/j.hrthm.2015.06.019

131. Antzelevitch C, Yan G-X. J-wave syndromes: Brugada and early repolarization syndromes. *Heart Rhythm* 2015;12:1852–1866. doi: 10.1016/j.hrthm.2015.04.014

132. Antzelevitch C, Brugada P, Brugada J, Brugada R, Shimizu W, Gussak I, Riera ARP. Brugada Syndrome. *Circ Res.* 2002;91:1114–1118.

133. Morita H, Nagase S, Kusano K, Ohe T. Spontaneous T wave alternans and premature ventricular contractions during febrile illness in a patient with Brugada syndrome. *J Cardiovasc Electrophysiol.* 2002;13:816–818. doi: 10.1046/j.1540-8167.2002.00816.x

134. Kirchhof P, Eckardt L, Rolf S, Esperer HD, Paul M, Wichter T, Klein HU, Breithardt G, Bocker D. T wave alternans does not assess arrhythmic risk in patients with Brugada syndrome. *Ann Noninvasive Electrocardiol.* 2004;9:162–165. doi: 10.1111/j.1542-474X.2004.92541.x

135. Tada T, Kusano KF, Nagase S, Banba K, Miura D, Nishii N, Watanabe A, Nakamura K, Morita H, Ohe T. Clinical significance of macroscopic T-wave alternans after sodium channel blocker administration in patients with Brugada syndrome. *J Cardiovasc Electrophysiol.* 2008;19:56–61. doi: 10.1111/j.1540-8167.2007.00967.x

136. Haissaguerre M, Cheniti G, Nademanee K, Sacher F, Duchateau J, Coronel R, Vigmond E, Boukens BJ, Bernus O. Dependence of epicardial T-wave on local activation voltage in Brugada syndrome. *Heart Rhythm* 2022;19:1686–1688. doi: 10.1016/j.hrthm.2022.05.036

137. Coronel R, Casini S, Koopmann TT, Wilms-Schopman FJG, Verkerk AO, de Groot JR, Bhuiyan Z, Bezzina CR, Veldkamp MW, Linnenbank AC, et al. Right ventricular fibrosis and conduction delay in a patient with clinical signs of brugada syndrome: A combined electrophysiological, genetic, histopathologic, and computational study. *Circulation* 2005;112:2769–2777.

138. Nademanee K, Raju H, Noronha SV, Papadakis M, Robinson L, Rothery S, Makita N, Kowase S, Boonmee N, Vitayakritsirikul V, et al. Fibrosis, connexin-43, and conduction abnormalities in the Brugada syndrome. *J Am Coll Cardiol.* 2015;66:1976–1986.

139. Weiss JN. Arrhythmias in Brugada syndrome: Defective depolarization, repolarization or both?. *JACC Clin Electrophysiol* 2021;7:271–272. doi: 10.1016/j.jacep.2020.12.020

140. Narayan SM, Bode F, Karasik PL, Franz MR. Alternans of atrial action potentials during atrial flutter as a precursor to atrial fibrillation. *Circulation* 2002;106:1968–1973. doi: 10.1161/01.cir.0000037062.35762.b4

141. Hiromoto K, Shimizu H, Furukawa Y, Kanemori T, Mine T, Masuyama T, Ohyanagi M. Discordant repolarization alternans-induced atrial fibrillation is suppressed by verapamil. *Circ J.* 2005;69:1368–1373. doi: 10.1253/circj.69.1368

142. Miyauchi Y, Zhou S, Okuyama Y, Miyauchi M, Hayashi H, Hamabe A, Fishbein MC, Mandel WJ, Chen LS, Chen P-S, et al. Altered atrial electrical restitution and heterogeneous sympathetic hyperinnervation in hearts with chronic left ventricular myocardial infarction. *Circulation* 2003;108:360–366. doi: 10.1161/01.CIR.0000080327.32573.7C

143. Watanabe I, Masaki R, Nuo M, Oshikawa N, Okubo K, Okumura Y, Ohya T, Yamada T, Saito S, Ozawa Y, et al. Effect of 60 minutes of rapid atrial pacing on atrial action potential duration in the in-situ canine heart. *J Interv Card Electrophysiol.* 2003;8:165–171. doi: 10.1023/a:1023909019945

144. Jousset F, Tenkorang J, Vesin J-M, Pascale P, Ruchat P, Rollin AG, Fromer M, Narayan SM, Pruvot E. Kinetics of atrial repolarization alternans in a free-behaving ovine model. *J Cardiovasc Electrophysiol.* 2012;23:1003–1012. doi: 10.1111/j.1540-8167.2012.02336.x

145. Verrier RL, Fuller H, Justo F, Nearing BD, Rajamani S, Belardinelli L. Unmasking atrial repolarization to assess alternans, spatiotemporal

heterogeneity, and susceptibility to atrial fibrillation. *Heart Rhythm* 2016;13:953–961. doi: 10.1016/j.hrthm.2015.11.019

146. Blatter LA, Kockskamper J, Sheehan KA, Zima AV, Huser J, Lipsius SL. Local calcium gradients during excitation-contraction coupling and alternans in atrial myocytes. *J Physiol.* 2003;546:19–31. doi: 10.1113/jphysiol.2002.025239

147. Pearman CM, Madders GWP, Radcliffe EJ, Kirkwood GJ, Lawless M, Watkins A, Smith CER, Trafford AW, Eisner DA, Dibb KM. Increased vulnerability to atrial fibrillation is associated with increased susceptibility to alternans in old sheep. *J Am Heart Assoc* 2018;7:e009972. doi: 10.1161/JAHA.118.009972

148. Lugo CA, Cantalapiedra IR, Peñaranda A, Hove-Madsen L, Echebarria B. Are SR Ca content fluctuations or SR refractoriness the key to atrial cardiac alternans?: insights from a human atrial model. *Am J Physiol Heart Circ Physiol.* 2014;306:H1540–H1552. doi: 10.1152/ajpheart.00515.2013

149. Chang KC, Trayanova NA. Mechanisms of arrhythmogenesis related to calcium-driven alternans in a model of human atrial fibrillation. *Sci Rep.* 2016;6:36395. doi: 10.1038/srep36395

150. Dibb KM, Clarke JD, Horn MA, Richards MA, Graham HK, Eisner DA, Trafford AW. Characterization of an extensive transverse tubular network in sheep atrial myocytes and its depletion in heart failure. *Circulation: Heart Failure.* 2009;2:482–489.

151. Frisk M, Koivumäki JT, Norseng PA, Maleckar MM, Sejersted OM, Louch WE. Variable T-tubule organization and Ca2+ homeostasis across the atria. *Am J Physiol Heart Circ Physiol.* 2014;307:H609–H620. doi: 10.1152/ajpheart.00295.2014

152. Brandenburg S, Kohl T, Williams GSB, Gusev K, Wagner E, Rog-Zielinska EA, Hebisch E, Dura M, Didié M, Gotthardt M, et al. Axial tube junctions control rapid calcium signaling in atria. *J Clin Invest.* 2016;126:3999–4015. doi: 10.1172/JCI88241

153. Guo D, Young L, Wu Y, Belardinelli L, Kowey PR, Yan G-X. Increased late sodium current in left atrial myocytes of rabbits with left ventricular hypertrophy: its role in the genesis of atrial arrhythmias. *Am J Physiol Heart Circ Physiol.* 2010;298:H1375–H1381. doi: 10.1152/ajpheart.01145.2009

154. Workman AJ, Marshall GE, Rankin AC, Smith GL, Dempster J. Transient outward K+ current reduction prolongs action potentials and promotes afterdepolarisations: a dynamic-clamp study in human and rabbit cardiac atrial myocytes. *J Physiol.* 2012;590:4289–4305. doi: 10.1113/jphysiol.2012.235986

155. Ono N, Hayashi H, Kawase A, Lin SF, Li H, Weiss JN, Chen PS, Karagueuzian HS. Spontaneous atrial fibrillation initiated by triggered activity near the pulmonary veins in aged rats subjected to glycolytic inhibition. *Am J Physiol Heart Circ Physiol.* 2007;292:H639–H648. doi: 10.1152/ajpheart.00445.2006

156. Baher AA, Uy M, Xie F, Garfinkel A, Qu Z, Weiss JN. Bidirectional ventricular tachycardia: Ping pong in the His-Purkinje system. *Heart Rhythm* 2011;8:599–605. doi: 10.1016/j.hrthm.2010.11.038

157. Suys B, De Paep R, Francois K, De Wolf D. Images in cardiovascular medicine. Concomitant T-wave alternans and pulsus alternans in a child with long-QT syndrome. *Circulation* 2003;108:e36. doi: 10.1161/01.CIR.0000079312.63225.AE

158. Schwartz PJ, Crotti L, Insolia R. Long-QT syndrome: from genetics to management. *Circ Arrhythm Electrophysiol* 2012;5:868–877.

159. Shu J, Li Y, Ju R, Yan G-X. Two Types of T Wave Alternans in Long-QT Syndrome. *J Cardiovasc Electrophysiol.* 2014;25:910–912. doi: 10.1111/jce.12427

160. Takasugi N, Goto H, Takasugi M, Verrier RL, Kuwahara T, Kubota T, Toyoshi H, Nakashima T, Kawasaki M, Nishigaki K, et al. Prevalence of microvolt T-wave alternans in patients with long QT syndrome and its association with torsade de pointes. *Circ Arrhythm Electrophysiol* 2016;9:e003206. doi: 10.1161/CIRCEP.115.003206

161. Pernot C. Le syndrome cardio-auditif de Jervell et Lange-Nielsen. Aspects electrocardiographiques. *Proc Ass Eur Paediat Cardiol.* 1972;8:28–36.

162. Goto H, Takasugi N, Kuwahara T, Verrier RL. QRST-wave alternans in a child with type 3 long-QT syndrome: an ominous ECG pattern appearing during transition from T-wave alternans to polymorphic VT. *J Cardiovasc Electrophysiol.* 2014;25:657–658. doi: 10.1111/jce.12354

163. Hanna EB, Ahmed J. Prolonged QT interval with T-wave alternans: electrocardiogram-based differential diagnosis. *Am J Med Sci.* 2013;346:128. doi: 10.1097/MAJ.0b013e318258f4a5

164. Cruz Filho FE, Maia IG, Fagundes ML, Barbosa RC, Alves PA, Sa RM, Boghossian SH, Ribeiro JC. Electrical behavior of T-wave polarity

alternans in patients with congenital long QT syndrome. *J Am Coll Cardiol.* 2000;36:167–173. doi: 10.1016/s0735-1097(00)00694-x

165. Cohen HC, D'Cruz I, Arbel ER, Langendorf R, Pick A. Tachycardia and bradycardia-dependent bundle branch block alternans: clinical observations. *Circulation* 1977;55:242–246. doi: 10.1161/01.cir.55.2.242

166. Rinkenberger RL, Polumbo RA, Bolton MR, Dunn M. Mechanism of electrical alternans in patients with pericardial effusion. *Cathet Cardiovasc Diagn* 1978;4:63–70. doi: 10.1002/ccd.1810040109

167. Kodama M, Kato K, Hirono S, Okura Y, Hanawa H, Ito M, Fuse K, Shiono T, Watanabe K, Aizawa Y. Mechanical alternans in patients with chronic heart failure. *J Card Fail.* 2001;7:138–145. doi: 10.1054/jcaf.2001.24122

168. Tempe DK, Garg M, Virmani S, Dutta D. An unusual arterial pressure waveform. *J Cardiothorac Vasc Anesth.* 2011;25:567–568. doi: 10.1053/j.jvca.2010.03.023

169. McLaughlin DP. Pulsus Alternans. *N Engl J Med.* 1999;341:955–955. doi: 10.1056/NEJM199909233411305

170. Aro AL, Kentta TV, Huikuri HV. Microvolt T-wave alternans: where are we now?. *Arrhythm Electrophysiol Rev* 2016;5:37–40. doi: 10.15420/aer.2015.28.1

171. Brockmeier K, Aslan I, Hilbel T, Eberle T, Ulmer HE, Lux RL. T-wave alternans in LQTS: repolarization-rate dynamics from digital 12-lead Holter data. *J Electrocardiol.* 2001;34:93–96. doi: 10.1054/jelc.2001.28838

172. Houltz B, DarpÖ B, Edvardsson N, BlomstrÖM PER, Brachmann J, Crijns HJGM, Jensen SM, Svernhage E, Vallin H, Swedberg K. Electrocardiographic and clinical predictors of torsades de pointes induced by almokalant infusion in patients with chronic atrial fibrillation or flutter: a prospective study. *Pacing Clin Electrophysiol.* 1998;21:1044–1057.

173. Nemec J, Hejlik JB, Shen W-K, Ackerman MJ. Catecholamine-induced T-wave lability in congenital long qt syndrome: A novel phenomenon associated with syncope and cardiac arrest. *Mayo Clin Proc.* 2003;78:40–50. doi: 10.4065/78.1.40

174. Donato A, Oreto G, Schamroth L. P wave alternans. *Am Heart J.* 1988;116:875–877. doi: 10.1016/0002-8703(88)90354-7

175. Pu JL, Balser JR, Boyden PA. Lidocaine action on Na+ currents in ventricular myocytes from the epicardial border zone of the infarcted heart. *Circ Res.* 1998;83:431–440. doi: 10.1161/01.res.83.4.431

176. Qu Z, Karagueuzian HS, Garfinkel A, Weiss JN. Effects of Na+ channel and cell coupling abnormalities on vulnerability to reentry: a simulation study. *Am J Physiol Heart Circ Physiol.* 2004;286:H1310–H1321. doi: 10.1152/ajpheart.00561.2003

177. Qian YW, Clusin WT, Lin SF, Han J, Sung RJ. Spatial heterogeneity of calcium transient alternans during the early phase of myocardial ischemia in the blood-perfused rabbit heart. *Circulation* 2001;104:2082–2087. doi: 10.1161/hc4201.097136

178. Epstein AE, Hallstrom AP, Rogers WJ, Liebson PR, Seals AA, Anderson JL, Cohen JD, Capone RJ, Wyse DG. Mortality following ventricular arrhythmia suppression by encainide, flecainide, and moricizine after myocardial infarction: The original design concept of the Cardiac Arrhythmia Suppression Trial (CAST). *JAMA* 1993;270:2451–2455.

179. Tachibana H, Yamaki M, Kubota I, Watanabe T, Yamauchi S, Tomoike H. Intracoronary flecainide induces ST alternans and reentrant arrhythmia on intact canine heart: A role of 4-aminopyridine-sensitive current. *Circulation* 1999;99:1637–1643. doi: 10.1161/01.cir.99.12.1637

180. Morita H, Morita ST, Nagase S, Banba K, Nishii N, Tani Y, Watanabe A, Nakamura K, Kusano KF, Emori T, et al. Ventricular arrhythmia induced by sodium channel blocker in patients with Brugada syndrome. *J Am Coll Cardiol.* 2003;42:1624–1631. doi: 10.1016/j.jacc.2003.06.004

181. Nishizaki M, Fujii H, Sakurada H, Kimura A, Hiraoka M. Spontaneous T wave alternans in a patient with Brugada syndrome—responses to intravenous administration of class I antiarrhythmic drug, glucose tolerance test, and atrial pacing. *J Cardiovasc Electrophysiol.* 2005;16:217–220. doi: 10.1046/j.1540-8167.2004.40411.x

182. Gao Y, Xue X, Hu D, Liu W, Yuan Y, Sun H, Li L, Timothy KW, Zhang L, Li C, et al. Inhibition of late sodium current by mexiletine: a novel pharmacotherapeutical approach in timothy syndrome. *Circ Arrhythm Electrophysiol* 2013;6:614–622. doi: 10.1161/CIRCEP.113.000092

183. Hashimoto H, Suzuki K, Miyake S, Nakashima M. Effects of calcium antagonists on the electrical alternans of the ST segment and on associated mechanical alternans during acute coronary occlusion in dogs. *Circulation* 1983;68:667–672. doi: 10.1161/01.cir.68.3.667

184. Hirayama Y, Saitoh H, Atarashi H, Hayakawa H. Electrical and mechanical alternans in canine myocardium in vivo. Dependence on intracellular

calcium cycling. *Circulation* 1993;88:2894–2902. doi: 10.1161/01.cir.88.6.2894

185. Luzza F, Oreto G. Verapamil-induced electrical and cycle length alternans during supraventricular tachycardia: what is the mechanism?. *J Cardiovasc Electrophysiol.* 2003;14:323–324. doi: 10.1046/j.1540-8167.2003.02463.x

186. Madhvani RV, Xie Y, Pantazis A, Garfinkel A, Qu Z, Weiss JN, Olcese R. Shaping a new Ca2+ conductance to suppress early afterdepolarizations in cardiac myocytes. *J Physiol.* 2011;589:6081–6092. doi: 10.1113/jphysiol.2011.219600

187. Zhang Z, Chen P-S, Weiss JN, Qu Z. Why is only type 1 electrocardiogram diagnostic of brugada syndrome? Mechanistic insights from computer modeling. *Circ Arrhythm Electrophysiol* 2022;15:e010365. doi: 10.1161/CIRCEP.121.010365

188. Waldo AL, Camm AJ, deRuyter H, Friedman PL, MacNeil DJ, Pitt B, Pratt CM, Rodda BE, Schwartz PJ; The SWORD Investigators. Survival with oral d-sotalol in patients with left ventricular dysfunction after myocardial infarction: rationale, design, and methods (the SWORD trial). *Am J Cardiol.* 1995;75:1023–1027.

189. Garfinkel A, Kim YH, Voroshilovsky O, Qu Z, Kil JR, Lee MH, Karagueuzian HS, Weiss JN, Chen PS. Preventing ventricular fibrillation by flattening cardiac restitution. *Proc Natl Acad Sci USA.* 2000;97:6061–6066. doi: 10.1073/pnas.090492697

190. Shimizu W, Kurita T, Matsuo K, Suyama K, Aihara N, Kamakura S, Towbin JA, Shimomura K. Improvement of repolarization abnormalities by a K+ channel opener in the LQT1 form of congenital long-QT syndrome. *Circulation* 1998;97:1581–1588. doi: 10.1161/01.cir.97.16.1581

191. Shimizu W, Antzelevitch C. Effects of a K+ channel opener to reduce transmural dispersion of repolarization and prevent Torsade de Pointes in LQT1, LQT2, and LQT3 models of the long-QT syndrome. *Circulation* 2000;102:706–712. doi: 10.1161/01.cir.102.6.706